

RESEARCH

Open Access

Steady state analysis of influx and transbilayer distribution of ergosterol in the yeast plasma membrane



Daniel Wüstner

Abstract

Background: The transbilayer sterol distribution between both plasma membrane (PM) leaflets has long been debated. Recent studies in mammalian cells and in yeast show that the majority of sterol resides in the inner PM leaflet. Since sterol flip-flop in model membranes is rapid and energy-independent, a mechanistic understanding for net enrichment of sterol in one leaflet is lacking. Import of ergosterol in yeast can take place via the ABC transporters Aus1/Pdr11 under anaerobic growth conditions, eventually followed by rapid non-vesicular sterol transport to the endoplasmic reticulum (ER). Little is known about how these transport steps are dynamically coordinated.

Methods: Here, a kinetic steady state model is presented which considers sterol import via Aus1/Pdr11, sterol flip-flop across the PM, bi-molecular complex formation and intracellular sterol release followed by eventual transport to and esterification of sterol in the ER. The steady state flux is calculated, and a thermodynamic analysis of feasibility is presented.

Results: It is shown that the steady state sterol flux across the PM can be entirely controlled by irreversible sterol import via Aus1/Pdr11. The transbilayer sterol flux at steady state is a non-linear function of the chemical potential difference of sterol between both leaflets. Non-vesicular release of sterol on the cytoplasmic side of the PM lowers the attainable sterol enrichment in the inner leaflet. Including complex formation of sterol with phospholipids or proteins can explain several puzzling experimental observations; 1) rapid sterol flip-flop across the PM despite net sterol enrichment in one leaflet, 2) a pronounced steady state sterol gradient between PM and ER despite fast non-vesicular sterol exchange between both compartments and 3) a non-linear dependence of ER sterol on ergosterol abundance in the PM.

Conclusions: A steady state model is presented that can account for the observed sterol asymmetry in the yeast PM, the strong sterol gradient between PM and ER and threshold-like expansion of ER sterol for increasing sterol influx into the PM. The model also provides new insight into selective uptake of cholesterol and its homeostasis in mammalian cells, and it provides testable predictions for future experiments.

Keywords: Sterol, Cholesterol, Ergosterol, Flip-flop, Plasma membrane, Flux, Non-equilibrium, Steady state, Esterification, Endoplasmic reticulum

Correspondence: wuestner@bmb.sdu.dk
Department of Biochemistry and Molecular Biology, VILLUM Center for Bioanalytical Sciences, University of Southern Denmark, Campusvej 55, DK-5230 Odense M, Denmark

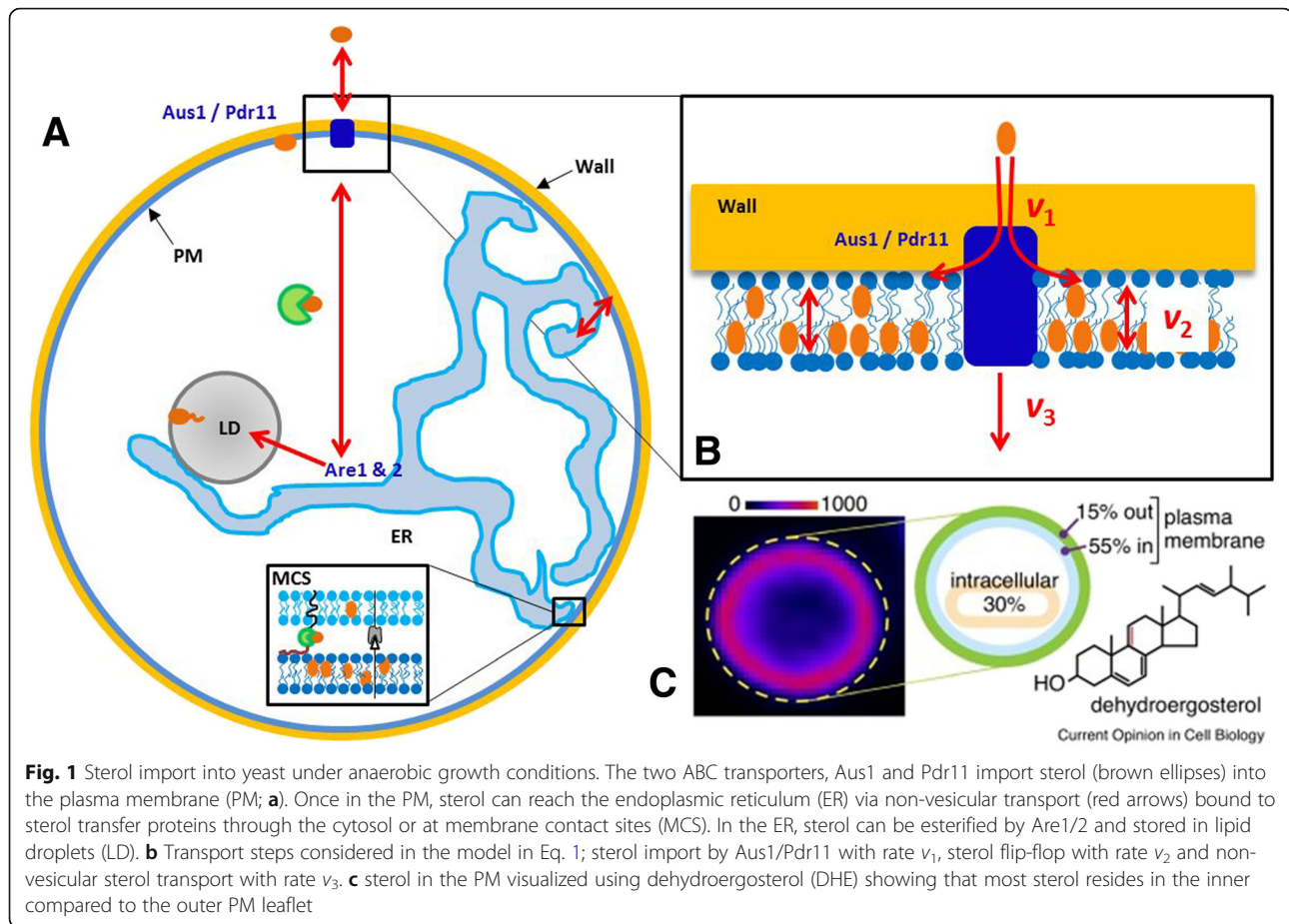


Background

Cells require sterols for growth and acquire these molecules from the extracellular medium or by de novo synthesis. Sterol transport in the bloodstream and uptake by cells is achieved with the participation of low density lipoprotein (LDL) receptors. While much information has been gathered about these processes, transport of sterols within cells is poorly understood [1–3]. Mammalian cells internalize cholesterol either by receptor mediated endocytosis of LDL or by selective sterol uptake processes. Selective sterol influx into the plasma membrane (PM) from circulating high density lipoprotein (HDL) is mediated by scavenger receptor BI (SR-BI) in the liver and gonads. Sterol import into the yeast PM takes place under anaerobic conditions and is mediated by ATP-dependent transport via the ABC transporters Aus1 and Pdr11 and potentially other transporters. In both, mammalian and yeast cells, intracellular sterol transport includes a non-vesicular pathway. In non-vesicular transport, sterol molecules are extracted from the cytoplasmic face of a ‘donor’ membrane by a carrier protein and off-loaded at the ‘acceptor’ compartment [4, 5]. Since sterols are very hydrophobic molecules, the thermodynamic sterol partition into the aqueous cytoplasm will be very low (on the order of $1\text{--}5\cdot 10^6$ in favor of the membrane) [6]. Due to its hydrophobicity and membrane condensing capacity, the activation energy for cholesterol to leave a lipid bilayer, E_A , is very high ($E_A \approx 75$ kJ/mol, that is 30fold $k_B\cdot T$) [6, 7]. Release rate constants have been directly measured from liposomes for dehydroergosterol (DHE), a fluorescent sterol differing from the natural yeast sterol ergosterol only by having one additional double bond [6]. The values were in the range of $k \approx 1\cdot 10^{-3} \text{ s}^{-1}$ for POPC ($t_{1/2} = 11.6$ min) over $6.4\cdot 10^{-4} \text{ s}^{-1}$ ($t_{1/2} = 18.1$ min) for a 1:1 mixture of POPC-cholesterol to $5\cdot 10^{-5} \text{ s}^{-1}$ ($t_{1/2} = 3.85$ h) for liposomes made of sphingomyelin-cholesterol, respectively [6]. Thus, sterol desorption depends on the bilayer lipid composition and is rate-limiting for overall passive sterol exchange between membranes [5, 8]. In contrast, transport of ergosterol between PM and ER in intact living yeast cells takes place with a half time of $t_{1/2} = 4\text{--}10$ min [9]. Thus, cells must have efficient mechanisms to speed up sterol exit from a bilayer for efficient non-vesicular sterol transport between organelle membranes. One possibility to guarantee intracellular non-vesicular sterol transport despite the low water solubility of sterols is the expression of sterol transport proteins (STPs) which lower E_A for sterol release from a membrane [5, 8]. Such STPs can be soluble cytoplasmic proteins which lower the free energy cost of sterol solvation by accommodating the released sterol in a hydrophobic

binding pocket. They can also be membrane proteins, containing two structural motifs, which anchor them simultaneously in the PM and in the ER, thereby creating close membrane contact sites (MCS) that may enhance the efficiency of STPs by confining them to a narrow space (Fig. 1) [10, 11]. The yeast *S. cerevisiae* contains ergosterol as main sterol, and many homologs to mammalian STPs have been discovered in this well-established model organism [12]. Recently discovered STPs include the oxysterol binding protein (OSBP) family, StART-like StARD4, Aster and GRAM proteins in mammalian cells as well as the related OSBP homologs (Osh) proteins and Lam proteins in yeast. These proteins have been implicated in non-vesicular sterol transport to the endoplasmic reticulum (ER), endosomes and to lipid droplets (LDs). Thus, allocation of sterol to the inner PM leaflet after selective uptake is necessary for its subsequent non-vesicular transport to various intracellular sites.

Rapid non-vesicular sterol transport between membranes raises the question, how cells can maintain strong sterol gradients between organelles at steady state [8, 10, 13]. It must mean that certain mechanisms ensure equal chemical potential of cholesterol in different cellular membranes despite varying concentrations. This, in turn, invokes membrane dependent activity coefficients due to specific interactions of sterols with other membrane components [8, 10, 13, 14]. Several observations made on regulation of cholesterol uptake and metabolism in mammalian cells can be rationalized with a model assuming two pool of cholesterol in the PM; active cholesterol is able to move freely between membranes by non-vesicular transport, while a second cholesterol pool forms stoichiometric complexes with other membrane components, such as phospho- and sphingolipids bearing saturated acyl chains [14–16]. In this model, cholesterol abundance in the PM sets a threshold for a sudden increase of active cholesterol once the capacity of the PM to form stoichiometric complexes is exceeded. Above this threshold, rapid flux of active cholesterol from the PM to the ER takes place within 10–15 min until cholesterol’s chemical potential in both membranes is equal again [10]. The sudden expansion of the sterol pool in the ER triggers feedback responses like activation of cholesterol esterification by acyl-Coenzyme A acyl transferase (ACAT) and shutdown of cholesterol synthesis via inhibition of the SCAP/INSIG/SREBP transcription factor complex [17–19]. This model has been also invoked to explain the strong ergosterol gradient between PM and ER in yeast despite continuous rapid non-vesicular sterol equilibration taking place in ca. 10 min [9, 20, 21]. It is not known how eventual sterol complex formation is kinetically regulated during sterol uptake and flip-flop in the PM, and no attempt has been made, so far,



to incorporate sterol complex formation in a steady state model of cellular sterol transport.

Sterol transport in yeast can be conveniently studied using live-cell imaging of the fluorescent DHE (Fig. 1c). DHE is a natural yeast sterol with comparable biophysical properties as ergosterol and cholesterol in model and cell membranes [22, 23]. DHE is like ergosterol taken up by yeast under anaerobic growth conditions, and its import into the yeast PM depends strictly on Aus1/Pdr11 [21, 24, 25]. In cells, lacking functional Aus1/Pdr11, DHE is not inserted into the PM but gets stuck in the cell wall from where it can be extracted using organic solvents [24]. Thus, these ABC transporters are necessary for insertion of sterol from the cell wall into the PM (see Fig. 1a, b). After shifting to aerobic conditions, DHE is internalized and partly esterified by sterol acyltransferases Are1 and 2 and deposited in lipid droplets (LD; Fig. 1a), exactly as ergosterol in wild-type cells [26, 27]. This can be quantified in kinetic imaging experiments relative to known organelle markers [27, 28]. Transport-coupled esterification of DHE is monitored in parallel [29, 30]. Recently, we

developed an assay for measuring the sterol transbilayer distribution in the PM of living yeast cells [31]. We used sterol-auxotroph yeast cells lacking Hem1 ($\Delta hem1$ cells), which makes them unable to use oxygen in ergosterol synthesis such that they can use DHE as only sterol source for growth and survival [27, 31]. In $\Delta hem1$ cells, ergosterol synthesis is eliminated and most DHE stays in the PM (Fig. 1c and [4, 31]). This allows for quantification of the transbilayer distribution of DHE in the PM using side-specific quenchers, which showed that up to 80% of DHE in the PM resides in its inner leaflet [31]. This asymmetric sterol distribution did not depend on metabolic energy, subcortical actin or a PM proton gradient. Sterol asymmetry across the PM required long-chain sphingolipids in the PM and was strongly reduced in cells lacking Drs2, a P-type ATPase transporting phosphatidylserine (PS) to the cytoplasmic leaflet of the PM and Golgi apparatus [31]. Since DHE and other sterols rapidly traverse model lipid membranes [32, 33], it is not clear how such a strong transbilayer sterol gradient can be established and maintained in the PM

of living cells. Similarly, exactly how cellular sterol import, sterol distribution between the two PM leaflets and non-vesicular intracellular sterol transport is coordinated, is not known.

Here, we have developed a mathematical steady state model for sterol import, sterol flip-flop across the yeast PM and cytoplasmic non-vesicular sterol transport. We derive analytical expressions, investigate their implications and suggest how they can be used for making concrete predictions in future experiments.

This paper is organized as follows; first, we introduce an irreversible model of sterol import with one sterol pool in each leaflet. We analyze the thermodynamics of the steady state flux for this model afterwards. Second, we extend this model by assuming reversible sterol import. Subsequently, a 2-pool model is introduced which accounts for sterol complex formation in the PM. This model is first discussed in a linearized version to develop key principles including sterol transport between PM and ER as well as sterol esterification in the ER. Next, this model is extended to account for biomolecular stoichiometric complex formation of sterol in the PM and ER, and the implications of this extension on sterol transport are discussed. Finally, results and predictions of our model are summarized and their implications for future experimental studies are discussed. Although developed for ergosterol transport in yeast, the model bears important implications for trafficking of cholesterol in mammalian cells. Accordingly, we refer also to cholesterol homeostasis in mammalian, wherever appropriate.

Methods

All calculations were carried out manually or with help of the Mathematica software (Wolfram Research Oxfordshire, UK). Analytical solutions were used for simulations using SigmaPlot (Systat Inc., Erkrath, Germany), which was also used for generating figures.

Results

Model of sterol transport in yeast with one sterol pool in each PM leaflet

Irreversible sterol import via Aus1/Pdr11 – steady state and control analysis

As a starting point for our discussion, we consider a simple model of sterol import in $\Delta hem1$ cells due to active transport by Aus1/Pdr11 with rate v_1 , sterol flip-flop with rate v_2 and sterol release from the inner PM leaflet to the ER with rate v_3 , where sterol is esterified (see Fig. 1b). Yeast cells are surrounded by a cell wall containing highly hydrated carbohydrates across which sterols cannot diffuse passively. Instead, sterol import requires the ABC transporters Aus1/Pdr11, which

mediate transport across the cell wall and likely direct sterol insertion into the PM outer leaflet [25, 4]. We assume that any sterol released from the PM is transported to the ER, where it is esterified by Are1 and Are 2 and stored as esters in LDs (Fig. 1a). This esterification process replenished by non-vesicular sterol release removes sterols from the PM and acts as permanent sink in our model. However, in this first modeling step, only the steady state flux across the PM is considered, while sterol arrival in the ER and sterol esterification are not explicitly taken into account, yet. These processes only enter the model at this stage via their effect on removing sterol released on the inner PM leaflet into the cytosol. This sterol removal is described by rate v_3 . Previous modeling work has shown that non-vesicular sterol transport by STPs is likely not limited by intracellular diffusion of sterol-protein complexes but rather by sterol pick up from the bilayer, at least in a physiologically relevant concentration range in small cells, like yeast [5]. Thus, concentration gradients of sterol-STP complexes in the cytoplasm can be ignored allowing for a simple ansatz using ordinary differential equations (ODEs) in our model. We have also not explicitly accounted for any volume effects to avoid extensive need for parametrization of our model. Accordingly, substance amounts and concentrations are often used synonymously. We have focused on the key features of coupled sterol import, transbilayer migration and cytosolic sterol release, allowing for a simple steady state description of the transport process. Being aware of possible non-ideal mixing of membrane sterols with phospholipids giving rise to membrane dependent activity coefficient of sterols, we nevertheless start out with a simple description using ideal solution theory. This is to obtain first insight into the underlying kinetic principles and steady state properties. Non-ideal behavior via sterol-phospholipid complexes is considered subsequently by extending the simpler kinetic model. Finally, we employ first-order kinetics by assuming that cytoplasmic STPs are not consumed in the sterol transfer reaction (i.e., $k_3 = k_3^* \cdot [STP]$, where the concentration of STPs, $[STP] = \text{constant}$). The extracellular sterol concentration, i.e. sterol in the medium, S_0 , is kept constant (clamped). This is realized in experiments by providing an excess supply of a tracer sterol (e.g. DHE) in Tween and oleic acid for 24-48 h, during which a steady state of sterol flux across the PM is established [31]. Alternatively, low amounts of sterol could be steadily supplied in a microfluidic device, thereby ensuring constant DHE levels in the medium. This model corresponds to the following kinetic scheme:



The corresponding differential equations for sterol in the outer PM leaflet (S_1) and the inner PM leaflet (S_2) read

with rates $v_1 = k_1 \cdot S_0$, $v_2 = k_2 \cdot S_1 - k_{-2} \cdot S_2$ and $v_3 = k_3 \cdot S_2$, respectively:

$$\begin{aligned} \frac{dS_1}{dt} &= v_1 - v_2 = k_1 \cdot S_0 - k_2 \cdot S_1 + k_{-2} \cdot S_2 \\ \frac{dS_2}{dt} &= v_2 - v_3 = k_2 \cdot S_1 - (k_{-2} + k_3) \cdot S_2 \end{aligned} \quad (2a, b)$$

The system (or Jacobian) matrix for the equations in (2a, b) contains the rate constants and has determinant $|A| = k_2 \cdot k_3 > 0$, indicating that we have a non-trivial steady state. As it is a linear system with negative real eigenvalues of A , this steady state is a stable fix point. The steady state amount of sterol in the outer and inner leaflet of the PM can be determined from Eq. 2a, b using Cramer's rule to:

$$\begin{aligned} \bar{S}_1 &= \frac{|A_1|}{|A|} = \frac{k_1 \cdot S_0 \cdot (k_{-2} + k_3)}{k_2 \cdot k_3} \\ &= \frac{v_1 \cdot (k_{-2} + k_3)}{k_2 \cdot k_3} \end{aligned} \quad (3a)$$

$$\bar{S}_2 = \frac{|A_2|}{|A|} = \frac{k_1 \cdot k_2 \cdot S_0}{k_2 \cdot k_3} = \frac{k_1 \cdot S_0}{k_3} = \frac{v_1}{k_3} \quad (3b)$$

Thus, the sterol amount in the inner leaflet at steady state is completely independent of the flip-flop rates, but solely determined by sterol insertion into and sterol release from the PM in this model. Using these expressions in (2a, b), we can find the steady state flux as:

$$\begin{aligned} \bar{v}_2 &= k_2 \cdot \bar{S}_1 - k_{-2} \cdot \bar{S}_2 = v_1 \\ \bar{v}_3 &= k_3 \cdot \bar{S}_2 = v_1 \end{aligned} \quad (4a, b)$$

Thus, the steady state flux through the PM is entirely determined by the influx via the ABC transporters Aus1/Prd11 in this model. In other words, the details of the sterol flip-flop mechanism do not impact the steady state flux of sterol from the medium into the cell. They do affect the kinetics of sterol import, though.

Based on these results, lets define the influx more properly. A reasonable assumption is that of an irreversible Michaelis-Menten-type kinetics, similar to glucose import by the GLUT transport system [34]:



Here, E is the amount of Aus1/Pdr11, acting as an enzyme for sterol import; m_1 and m_{-1} are the association and dissociation rate constants for sterol in the medium (S_0) and Aus1/Pdr11 at the outer side of the cell, respectively. The catalyzed insertion of sterol into the outer leaflet is modeled with rate constant m_2 . This leads with the classical quasi-steady state assumption for the ES_0 complex to the well-known hyperbolic Michaelis-Menten type law for sterol import rate (v_1^{MM}):

$$v_1^{MM} = \frac{v_{\max} \cdot S_0}{k_M + S_0} \quad (6)$$

Here, v_{\max} is the maximal transport rate of the Aus1/Pdr11 transport system ($=m_2 \cdot E_T$, with E_T being the total amount of Aus1/Pdr11 transporters in the PM), and the Michaelis-Menten constant is $k_M = \frac{m_{-1} + m_1}{m_2}$. With that, we can express the steady state flux into the cell as function of the kinetic parameters of the Aus1/Pdr11 transport system. The hyperbolic kinetics of sterol uptake by Aus1/Pdr11 can be linearized for two extreme cases:

Low-substrate range In the low-substrate regime, i.e., for low external sterol, Eq. 6 can be linearized according to:

$$v_{1,lin}^{MM} = \left. \frac{\partial v_1^{MM}}{\partial S_0} \right|_{S_0 \rightarrow 0} \cdot S_0 = \frac{v_{\max}}{k_M} \cdot S_0 = k_1 \cdot S_0 = v_1 \quad (7)$$

Thus, for low amounts of sterol in the medium, a linearization of the irreversible import model recovers the rate constant k_1 from the differential equation system in Eq. 2a, b with $k_1 \cdot S_0 = \frac{v_{\max}}{k_M} \cdot S_0 = \frac{m_1 \cdot E_T}{k_M} \cdot S_0$. This situation could apply when using a microfluidic device to ensure a constant but low supply of ergosterol or its fluorescent analogue DHE. One could also use highly fluorescent tagged analogues of cholesterol, like nitro-benzoxadiazole (NBD)-tagged cholesterol, for which a steady supply of trace amounts would be sufficient to achieve sufficient staining of cells [35, 36]. Finally, one could express mutants of Aus1/Pdr11 or use inhibitors, which both impact the binding of sterol substrate to the transporters, thereby increasing their k_M values and shifting the linear regime of the hyperbolic Michaelis-Menten kinetics to higher substrate values. For this linear substrate-transport relationship, we ask how an infinitesimal change in the enzyme parameters of Aus1/Pdr11 will affect the steady state flux of sterol into the cell. To answer that, we use the fact that at steady state, we have $v_1 = k_1 \cdot S_0 = \bar{v}_2 = \bar{v}_3 = \bar{v}_1 = J$ and calculate the flux control coefficients, a measure quantifying the impact of infinitesimal parameter changes on the steady state flux [37]. The only non-trivial flux control coefficient is:

$$C_{k_1}^J = \frac{k_1}{J} \cdot \frac{\partial J}{\partial k_1} = 1 \quad (8)$$

All other flux control coefficients are zero. Thus, the total control about sterol flux into the cell lies in the ATP-driven sterol import process in our model, and a small change in the activity or abundance of Aus1/Pdr11 should directly translate into a proportional change in sterol import flux and sterol abundance in both leaflets. This conclusion, however, is only valid, as long as we

consider linear kinetics and infinitesimal changes in the parameter values for the import process.

In a similar manner, we can calculate concentration control coefficients, generally defined as [37]:

$$C_k^{S_i} = \left(\frac{v_k \Delta S_i}{S_i \Delta v_k} \right)_{\Delta v_k \rightarrow 0} = \frac{v_k \partial S_i / \partial p_k}{S_i \partial v_k / \partial p_k} = \frac{\partial \ln S_i}{\partial \ln v_k} \quad (9)$$

For sterol in the outer leaflet, changing the import rate constant, for example by altering the catalytic activity or abundance of Aus1/Pdr11 or by slightly changing the sterol amount in the medium will give:

$$\begin{aligned} C_J^{\bar{S}_1} &= \frac{J}{\bar{S}_1} \cdot \frac{\partial \bar{S}_1}{\partial J} = \frac{k_1 \cdot S_0 \cdot k_2 \cdot k_3}{k_1 \cdot S_0 \cdot (k_{-2} + k_3)} \frac{(k_{-2} + k_3)}{k_2 \cdot k_3} \\ &= 1 \end{aligned} \quad (10)$$

Similarly, one can show that the control over the steady state amount of sterol in the inner leaflet is entirely set by the sterol import process, i.e., one gets $C_J^{\bar{S}_2} = 1$. Thus, total steady state amounts of sterol in the outer and inner leaflet, respectively, follow changes in the sterol import step in a concerted manner.

High-substrate range In the high-substrate range (i.e., for $S_0 \rightarrow \infty$), Eq. 7 gives $v_1^{MM} = v_{max}$, i.e., sterol excess in the medium would make that the Aus1/Pdr11 transport system is always saturated and works under its maximal capacity. In that situation, sterol import becomes independent of the actual sterol concentration in the medium. Recently, we carried out ergosterol uptake experiments using its close analog DHE in *hem1Δ* cells [31]. Experiments on uptake of the ergosterol analogue DHE had been conducted in log-phase growing yeast with OD600 around 0.75 corresponding to $1.16 \cdot 10^7$ cells/ml. To these cells 20 μg/ml DHE in Tween had been added, which equals a concentration of 50.68 μM [31]. Thus, translated into our model, we have $S_0 = 50.68 \mu\text{M}$. After 24-48 h culture, all ergosterol in the cells had been replaced by DHE [31]. A yeast cell has about $1 \cdot 10^8$ ergosterol molecules [20], thus, there are $1.16 \cdot 10^{15}$ DHE molecules/ml incorporated into the cells in the 1-ml suspension, corresponding to 1.926 μM. Accordingly, DHE in the medium is in large (>25fold) excess of DHE in the cells, which corresponds to situation b), in which $v_1 = v_{max}$. Thus, uptake becomes independent of DHE abundance in the medium (0. order kinetics), and the steady state flux is entirely set by the maximal capacity of the sterol import system Aus1/Pdr11. This corresponds to a constant (clamped) concentration S_0 . Since $v_{max} = m_2 \cdot E_T$, the expression level of Aus1/Pdr11 transporters in the PM, E_T , translates in this case

directly into the magnitude of sterol flux across the yeast PM at steady state. There are about $10.5 \cdot 10^3$ Aus1 transporters per yeast cell (<http://yeastgenome.org/>), which corresponds to $12.18 \cdot 10^{13}$ transporters per l, equal to $2.02 \cdot 10^{-10}$ mol/l. Thus, one can estimate $E_T = 0.2$ nmol/l for the DHE uptake experiments carried out previously [4, 31]. Furthermore, the catalytic efficiency of purified and reconstituted Aus1/Pdr11 has been estimated to hydrolysis of 10 ATP molecules per protein per second, thus 0.167 ATP's per sec [38, 39]. Assuming that the catalytic efficiency is the same in intact cells and that there is a 1:1 stoichiometric coupling between sterol transport and ATP-hydrolysis by these ABC transporters, one gets $m_2 = 0.167$ transported sterol molecules per sec. Thus, we arrive at $v_{max} = 0.033$ nmol/(l·s) as the maximal possible capacity of the sterol influx system in our yeast cell culture. Is this a reasonable number? As a test, we ask how long it would take to reach a steady state DHE labeling of 1.926 μM (see above) with this flux magnitude, which gives 1926 nmol/l: $0.033 \text{ nmol}/(\text{l}\cdot\text{s}) = 58363,6 \text{ s} \approx 16 \text{ h}$. This value is comparable to the 24-h sterol labeling procedure, which we typically used. Thus, we conclude that these numbers are very reasonable.

Intracellular sterol release affects the transbilayer sterol distribution in the PM

Exit of sterol from the cytoplasmic leaflet is supposed to be an important control point in setting the sterol content of the ER and thereby regulating overall sterol homeostasis in both, yeast and mammalian cells [13, 14]. Release of cholesterol from the PM of mammalian cells is supposed to be rather slow compared to transbilayer sterol flip flop under normal growth conditions resulting for example in bi-phasic transport to the endocytic recycling compartment in fibroblasts [40]. Acute cholesterol loading, intercalation of membrane active molecules or depletion of sphingolipids can result in a non-linear increase of cholesterol release from the PM and thereby acute expansion of the cholesterol pool in the ER and other organelles [41–44]. In yeast, exit of the fluorescent ergosterol analogue DHE from the PM is low under anaerobic growth conditions but can be enhanced several fold after switching to aerobic growth, likely because newly made ergosterol can replace some DHE in the PM [20, 27, 31]. Here, more DHE is made available for pick up by cytosolic STPs, thereby increasing the rate of non-vesicular transport of DHE from the PM to the ER. In the ER, the sterol get esterified and stored in lipid droplets, which was found to require metabolic energy and activity of the yeast ACAT homologue, Are2 [27]. Thus, in both yeast and

mammalian cells, sterol exit from the PM seems to depend on active sterol esterification. In our model of Eq. 1, sterol exit from the PM and its esterification in the ER is summarized by rate $v_3 = k_3 \cdot S_2$, and a relevant question is, how this rate affects the steady state ratio of sterol in the PM. This reads:

$$\begin{aligned} \overline{S_2}/\overline{S_1} &= \frac{v_1}{k_3} \cdot \frac{k_2 \cdot k_3}{v_1 \cdot (k_{-2} + k_3)} = \frac{k_2}{k_{-2} + k_3} \\ &= \frac{q_2}{1 + k_3/k_{-2}} = Q \end{aligned} \quad (11)$$

Here, q_2 is the equilibrium constant of the sterol flip-flop process, i.e., $q_2 = \frac{k_2}{k_{-2}} = \frac{S_2^{eq}}{S_1^{eq}}$, where S_1^{eq} and S_2^{eq} are the sterol concentration at equilibrium in the outer and inner leaflet, respectively. Thus, we see that the steady state ratio of sterol between inner and outer leaflet, Q , is independent of the steady state sterol influx, v_1 . In fact, Q is described by a ratio of rate constants making that it has no units. Accordingly, the absolute values of kinetic rate constants are not relevant in making predictions about the steady state sterol ratio in the PM, only their relationship to each other. This is important as such values are not known for membranes in living cells. We see that Q is always smaller than the equilibrium ratio, i.e., as long as k_3 , the rate constant describing sterol exit from the PM is larger than zero. But how much does cytoplasmic sterol release affect this ratio or is the effect negligible under physiological settings? In case of $k_3 = 0$, one finds again the equilibrium sterol distribution across the PM (i.e., in this case $Q = q_2$). In Fig. 2a, the relationship between the equilibrium constant for passive sterol transbilayer distribution, q_2 , is plotted versus the steady state ratio, Q for varying release rate constants of sterol from the inner leaflet. For this calculation, the rate constant for sterol migration from the inner to the outer PM leaflet (sterol flopping) was set to $k_{-2} = 0.1 \text{ s}^{-1}$, while that in the opposite direction (sterol flipping) was varied between $k_2 = 0.01\text{--}1.0 \text{ s}^{-1}$, corresponding to an equilibrium ratio of $q_2 = 0.1\text{--}10$. Sterol release from the cytoplasmic leaflet was also varied over a 100fold range from $k_3 = 0.01\text{--}1.0 \text{ s}^{-1}$. One can see that for $k_3 = 0.01 \text{ s}^{-1}$, which is 10fold smaller than the flop rate constant k_{-2} , the attainable steady state ratio of sterol in the two PM leaflets closely resembles the equilibrium distribution (Fig. 2a, black curve). In contrast, already when $k_3 = 0.05 \text{ s}^{-1}$ equal to half the rate constant for sterol flopping, Q deviates significantly from q_2 , and this difference grows as k_3 is increased. To illustrate this further, we plotted the percentage of sterol in the inner leaflet for the same parameter

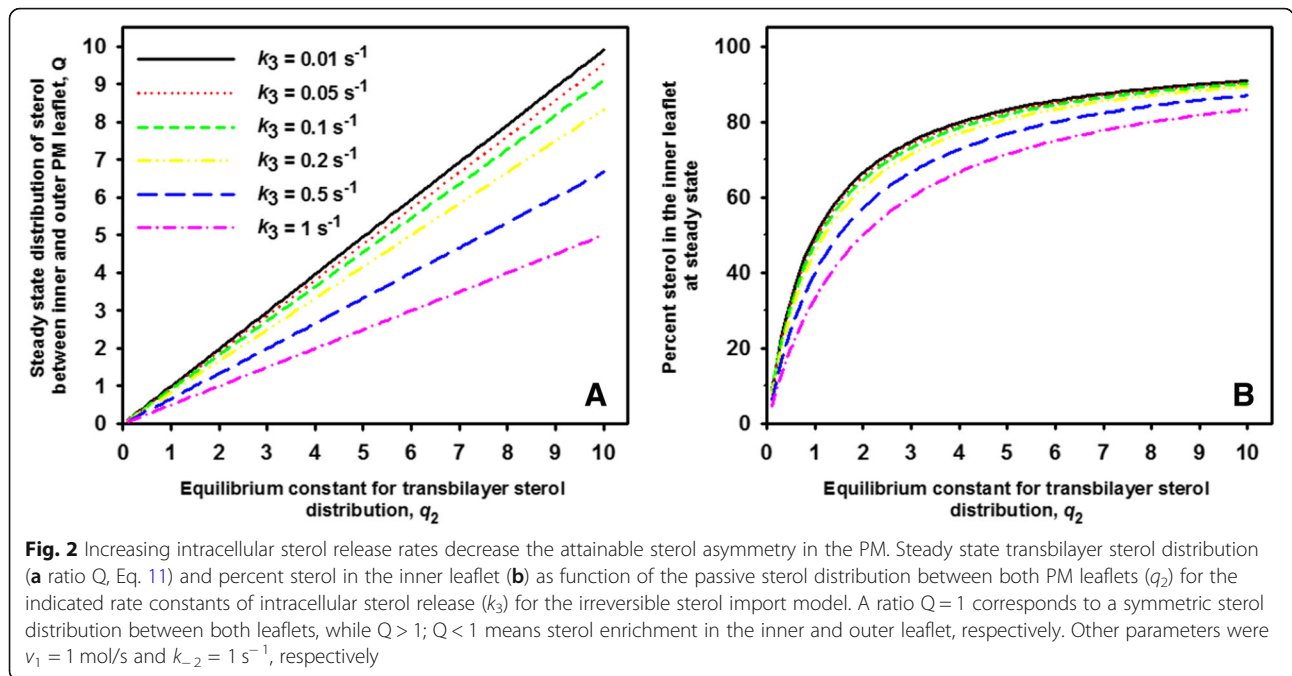
values (Fig. 2b). One finds that the experimentally measured ~79% sterol in the inner leaflet of *hem1Δ* cells at steady state [31] requires $q_2 = 4.2$ for a release rate constant of $k_3 = 0.01 \text{ s}^{-1}$ corresponding to a passive equilibrium distribution of 80.77% sterol in the inner leaflet. Thus, the percentage of sterol in the inner leaflet at steady state (79%) is almost identical to the passive sterol distribution at thermodynamic equilibrium (~81%) for this parameter combination, and such small differences cannot be detected in experiments [31]. In contrast, for a 10fold higher release rate constant of $k_3 = 0.1 \text{ s}^{-1}$, to obtain 79% sterol in the inner leaf of the PM at steady state requires $q_2 = 7.5$, i.e. a passive equilibrium distribution of 88.23% sterol in the inner leaflet. At the same time, such increased sterol release on the cytosolic side would lower the total amount of sterol in the PM by about 10 fold (Fig. 3a). This is a rather drastic change, which has not been observed in experiments [31]. Thus, one might wonder under which physiological conditions the steady state sterol distribution in the PM would differ significantly from the equilibrium distribution. In other words, does the in vivo situation more resemble a state in which flip-flop is much faster than cytoplasmic sterol release and esterification in the ER? In this case, one would always have $k_3 \ll k_2, k_{-2}$ and expect that Q approaches the equilibrium sterol transbilayer distribution. This is further analyzed in the thermodynamic analysis below.

Irreversible sterol import via Aus1/Pdr11 – thermodynamic analysis

To assess the extent by which continuous ergosterol import into yeast causes an out-of-equilibrium sterol distribution in the PM, we explored how the kinetic parameters affect the thermodynamic driving force for sterol influx. We define first the chemical potential difference of sterol between both leaflets under standard conditions in equilibrium

$$\Delta\mu^0 = \mu_2^0 - \mu_1^0 = RT \cdot \ln\left(\frac{1}{q_2}\right) \quad (12)$$

It has been suggested that the chemical potential of sterol in both leaflets at steady state is not the same, and that especially the higher content of phosphatidylethanolamine could ‘draw’ sterol to the inner leaflet, establishing that $q_2 = k_2/k_{-2} > 1$ [45]. In addition, there is a non-equilibrium contribution to the asymmetric sterol distribution in the PM and for that, we define the chemical potential difference at steady state as:

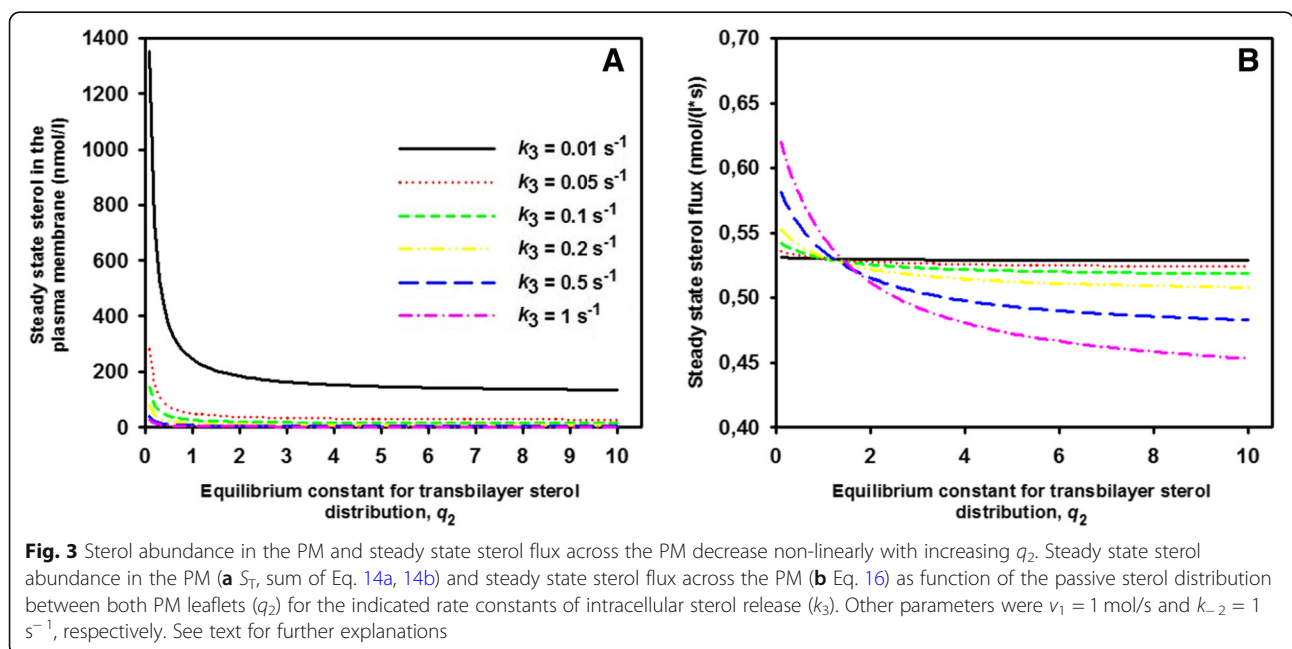


$$\begin{aligned} \Delta\mu &= \Delta G = \mu_2 - \mu_1 = \Delta\mu^0 + RT \cdot \ln\left(\frac{\bar{S}_2}{\bar{S}_1}\right) \\ &= -RT \cdot \ln\left(\frac{\bar{v}_2^+}{\bar{v}_2^-}\right) = RT \cdot \ln\left(\frac{\bar{v}_2^-}{\bar{v}_2^+}\right) \end{aligned} \quad (13)$$

$\cdot S_0 = \bar{v}_2^+ - \bar{v}_2^-$, for the low-substrate regime and $J = v_1 = v_{\max} = \bar{v}_2^+ - \bar{v}_2^-$ for the high-substrate regime, which is easily verified using Eq. 3a, 3b. Using $S_T = \bar{S}_1 + \bar{S}_2$, we can rewrite Eq. 3a, 3b as:

Here, the steady state forward (flip) and reverse rate (flop) for the transbilayer migration of sterol is defined as $\bar{v}_2^+ = k_2 \cdot \bar{S}_1$ and $\bar{v}_2^- = k_{-2} \cdot \bar{S}_2$, where we have $J = v_1 = k_1$

$$\bar{S}_1 = \frac{k_{-2} \cdot S_T + J}{k_2 + k_{-2}} \quad (14a)$$



$$\bar{S}_2 = \frac{k_2 \cdot S_T - J}{k_2 + k_{-2}} \tag{14b}$$

With that, the chemical potential difference for sterol between both leaflets at steady state (Eq. 13) reads:

$$\begin{aligned} \Delta\mu &= -RT \cdot \ln \left(\frac{(k_{-2} \cdot S_T + v_1)}{(k_2 \cdot S_T - v_1)} \cdot q_2 \right) = \Delta G \\ &= RT \cdot \ln \left(\frac{S_1^{eq} \cdot \bar{S}_2}{S_2^{eq} \cdot \bar{S}_1} \right) = RT \cdot \ln \left(\frac{Q}{q_2} \right) \end{aligned} \tag{15}$$

The expression in the large brackets in the right-hand term of Eq. 15 can be seen as a form of the mass action ratio for a non-equilibrium system (i.e. Q/q_2). With that, we can express the steady state flux as function of the chemical potential difference of sterol between the PM leaflets [46]:

$$J = \frac{k_2 \cdot S_T \cdot (\exp(-\Delta\mu/RT) - 1)}{q_2 + \exp(-\Delta\mu/RT)} \tag{16}$$

This thermodynamic definition of the steady state flux is valid for linear import kinetics. In that case, sterol influx necessary to counterbalance a non-equilibrium difference in sterol abundance between both leaflets is a monotonically decreasing non-linear function of the equilibrium sterol distribution between both leaflets (Fig. 3b). That is, the higher the passive sterol distribution towards the inner PM leaflet, the lower is the steady state sterol flux into the cell. In other words, the faster sterols flip spontaneously across the PM compared to cytoplasmic sterol release the closer is the system to thermodynamic equilibrium. Vice versa, higher sterol chemical potential differences due to large sterol release from the inner leaflet and esterification in the ER, as described by rate constant k_3 , result in larger steady state fluxes (e.g. compare pink dot-dashed curve with $k_3 = 1 \text{ s}^{-1}$ and green dashed curve with $k_3 = 0.1 \text{ s}^{-1}$ in Fig. 3b). The rate constant k_3 in the model of Eq. 1 comprises cytoplasmic sterol release and its esterification in the ER. Consequently, controlling the ‘sterol sink’ in the ER, i.e. sterol esterification by Are2 should directly relate to the magnitude of out-of-equilibrium sterol flux across the PM. Positive values of $\Delta\mu$ would give a negative flux, i.e., a flux reversion from the inner towards the outer leaflet. However, such a situation cannot happen, as long as we have $k_3 \geq 0$. This can be easily seen, when using Eq. 11, in Eq. 15 to get:

$$\begin{aligned} \Delta G = \Delta\mu &= RT \cdot \ln \left(\frac{Q}{q_2} \right) \\ &= RT \cdot \ln \left(\frac{1}{1 + k_3/k_{-2}} \right) \end{aligned} \tag{17}$$

For $k_3 = 0$, we get $\Delta G = 0$, which is the thermodynamic equilibrium. In that situation we have $\bar{v}_2^+ = \bar{v}_2^-$, meaning that no net flux across the PM would remain. So, how different is the ergosterol distribution between the two PM leaflets at a physiologically reasonable steady state from its equilibrium value? Again, the total number of ergosterol molecules in the PM is $S_T = 7 \cdot 10^7$ per yeast cell. Even though this is widely speculative, let’s assume that passive sterol flip and flop have a half time of $t_{1/2} = 1.73 \text{ s}$ ($k_2 = 0.4 \text{ s}^{-1}$) and $t_{1/2} = 6.93 \text{ s}$ ($k_{-2} = 0.1 \text{ s}^{-1}$), respectively. This corresponds to a passive distribution of sterol between the outer and inner PM leaflet of $q_2 = 4$ and thereby to 20% of ergosterol ($1.4 \cdot 10^7$ molecules) in the outer and 80% ($5.6 \cdot 10^7$ molecules) in the inner PM leaflet at thermodynamic equilibrium (i.e. in the absence of any intracellular sterol release from the PM described by rate constant k_3). In the presence of a cytoplasmic release from the PM with rate constant of $k_3 = 0.01 \text{ s}^{-1}$ ($t_{1/2} = 69 \text{ s}$), $7 \cdot 10^5$ ergosterol molecules would leave the PM per second. With that, we have according to Eqs. 15 and 16 at steady state $Q = \frac{\bar{S}_2}{\bar{S}_1} = 3.64$, thus, 21.56% of ergosterol ($1.51 \cdot 10^7$ molecules) in the outer and 78.44% ($5.49 \cdot 10^7$ molecules) in the inner leaflet at steady state. This is only slightly different from the equilibrium situation, above. Such a difference is too small to be detectable in a steady state quenching experiment of DHE in the yeast PM, for example [31]. Supporting this notion, we found that energy poisoning of cells did not affect the measured distribution of DHE across the yeast PM [31]. For these values, we get for the Gibbs free energy:

$$\begin{aligned} \Delta G &= RT \cdot \ln \left(\frac{1}{1 + k_3/k_{-2}} \right) \\ &= RT \cdot \ln \left(\frac{1}{1 + 0.01 \text{ s}^{-1} / 0.1 \text{ s}^{-1}} \right) \\ &= -0.24 \text{ kJ/mol} \end{aligned} \tag{18}$$

This value of $\Delta G = -0.24 \text{ kJ/mol}$ is a rather low thermodynamic driving force, and the system will remain close to thermodynamic equilibrium. Let’s increase the rate constant for sterol release from the inner leaflet, k_3 , 5fold, i.e., from $k_3 = 0.01 \text{ s}^{-1}$ to $k_3 = 0.05 \text{ s}^{-1}$ while keeping $q_2 = 4.0$ with a sterol flip and flop rate constant of $k_2 = 0.4 \text{ s}^{-1}$ and $k_{-2} = 0.1 \text{ s}^{-1}$, respectively. This corresponds to $\Delta G = -1.03 \text{ kJ/mol}$. Again, this value for the Gibbs free energy change would also be obtained for very different values of the rate constants, as long as their ratio is the same. For example, one might have in a yeast cell, $k_2 = 0.04 \text{ s}^{-1}$ ($t_{1/2} = 17.3 \text{ s}$) and $k_{-2} = 0.01 \text{ s}^{-1}$ ($t_{1/2} = 69.3 \text{ s}$). In that case, the above example calculations stay valid for $k_3 = 0.001 \text{ s}^{-1}$ ($t_{1/2} = 693.2 \text{ s}$) to $k_3 = 0.005 \text{ s}^{-1}$ ($t_{1/2} = 138.6 \text{ s}$). This is important, as the

absolute values for sterol flip-flop, for example, have been debated and might vary over a wide range depending on lipid composition [47].

In parallel, we get using Eqs. 11 and 17; $Q = \frac{\overline{S_2}}{S_1} = 0.4 \text{ s}^{-1} / (0.1 \text{ s}^{-1} + 0.05 \text{ s}^{-1}) = 0.04 \text{ s}^{-1} / (0.01 \text{ s}^{-1} + 0.005 \text{ s}^{-1}) = 2.67$ (i.e. 72.75% sterol in the inner leaflet). Such a change in sterol asymmetry might be detectable by DHE quenching experiments. However, at the same time the total amount of sterol in the PM would drop to less than 20% of what it was at $k_3 = 0.01 \text{ s}^{-1}$ (for $k_2 = 0.1 \text{ s}^{-1}$) and at $k_3 = 0.001 \text{ s}^{-1}$ (for $k_2 = 0.01 \text{ s}^{-1}$) This, again, has not been observed in experiments, at least not in the absence of de novo ergosterol synthesis [27, 28, 31]. Thus, we can conclude that cytoplasmic release of ergosterol is likely slow compared to sterol flip-flop rates (i.e. $k_{-2} \geq 10 \cdot k_3$) causing only moderate deviations from the equilibrium sterol distribution in the PM.

For such small deviations from equilibrium, we can linearize the flux-force relationship of Eq. 16 and get [46]:

$$J = -\Delta\mu \cdot \frac{S_T}{RT} \cdot \left(\frac{k_2 \cdot k_{-2}}{k_2 + k_{-2}} \right) = -\Delta\mu \cdot \frac{S_T \cdot k_2}{RT(q_2 + 1)} \quad (19)$$

This resembles the Onsager flux force relationship for linear irreversible thermodynamics; $J = L \cdot X$, with the steady state flux being $J = v_1$, X being the driving force (here $X = -\Delta\mu$) and L being the transport coefficient (or ‘conductance’ (equivalent to a diffusion constant), here:

$$L = \frac{S_T \cdot k_2}{RT(q_2 + 1)} = \frac{S_T \cdot k_2 \cdot k_{-2}}{RT \cdot \tau} \quad (20)$$

With $S_T = [v_1 \cdot (\tau^{-1} + k_3)] / [k_2 \cdot k_3]$ the ‘conductance’ is determined by a combination of all rate constants of sterol transport across the PM relative to the Boltzmann factor (the higher the flip-flop rates, the faster is sterol exchange; where $\tau = (k_2 + k_{-2})^{-1}$ is the fluctuation relaxation time). From that, we can derive the heat loss due to entropy production, σ , per unit membrane area as [46]:

$$T \cdot \sigma = J \cdot X = -\Delta\mu \cdot v_1 = (\Delta\mu)^2 \cdot \frac{S_T \cdot k_2 \cdot k_{-2}}{RT \cdot \tau} \quad (21)$$

Thus, the larger the sterol flux across the PM, the higher is the entropy production, as expected for a non-equilibrium steady state. Again, based on the above quantitative arguments, we expect the flux to be small causing only small deviations from thermodynamic equilibrium distributions. The directionality of this steady state influx is ensured by Aus1/Pdr11 transporters constantly hydrolyzing ATP. Can we include this in our analysis?

Reversible sterol import via Aus1/Pdr11 – steady state analysis

It is generally believed that ABC transporters shuttle their substrate in an unidirectional manner driven by ATP hydrolysis. However, some of those transporters like the LmrA multidrug transporter of *Lactococcus lactis* can act also in the opposite direction under ATP depletion condition and reversed substrate gradients [48]. While the simultaneous existence of a reverse sterol and ATP gradient to synthesize ATP by Aus1/Pdr11 in yeast is rather implausible, the possibility exists that the ABC transporters Aus1/Pdr11 could carry out a reversible transport cycle. In this scenario, the ABC transporters could pump sterols also out of the cell, but the excess of ATP compared to ADP and phosphate on the substrate-entry site would ensure the directionality of sterol flux in the import direction [46]. Such a mechanism has been proposed for the ABC transporter associated with antigen processing (TAP) [49]. In that case, we have for our system:



We consider sterol in the outer PM leaflet (S_1) and the inner PM leaflet (S_2) with constant concentration of ATP, ADP and phosphate, i.e. $A := [\text{ATP}]$ and $P := [\text{ADP}] \cdot [\text{PO}_4^{2-}]$ and the rates $v_1 = k_1^* \cdot S_0 - k_{-1}^* \cdot S_1$, $v_2 = k_2 \cdot S_1 - k_{-2} \cdot S_2$ and $v_3 = k_3 \cdot S_2$ resulting in pseudo-first order rate constants for the import as $k_1^* = k_1 \cdot A$ and $k_{-1}^* = k_{-1} \cdot P$. This gives the ODE system:

$$\begin{aligned} \frac{dS_1}{dt} &= v_1 - v_2 = k_1^* \cdot S_0 - (k_{-1}^* + k_2) \cdot S_1 + k_{-2} \cdot S_2 \\ \frac{dS_2}{dt} &= v_2 - v_3 = k_2 \cdot S_1 - (k_{-2} + k_3) \cdot S_2 \end{aligned} \quad (23a, b)$$

One can again show, that only one steady state flux exists, which is $v_1 = v_2 = v_3 = J$. Thus, sterol fluxes due to i) Aus1/Pdr11-mediated sterol influx (v_1), ii) sterol flip-flop across the PM (v_2), and iii) due sterol release from the PM followed by sterol esterification in the ER (v_3) become equal at steady state. The steady state amount of sterol in the outer and inner leaflet of the PM reads:

$$\overline{S_1} = \frac{k_1 \cdot S_0 \cdot (k_{-2} + k_3)}{k_{-1}^* \cdot k_{-2} + (k_{-1}^* + k_2) \cdot k_3} \quad (24a)$$

$$\overline{S_2} = \frac{k_1 \cdot k_2 \cdot S_0}{k_{-1}^* \cdot k_{-2} + (k_{-1}^* + k_2) \cdot k_3} \quad (24b)$$

These expressions can be adapted for the high-substrate regime (b) by replacing $v_1 = k_1 \cdot S_0$ with $v_1 = v_{\max}$.

Importantly, the steady state ratio of sterol between the two PM leaflets is again independent of the activity or abundance of Aus1/Pdr11, as it reads:

$$\begin{aligned} \overline{S_2}/\overline{S_1} &= \left(\frac{k_1 \cdot k_2 \cdot S_0}{k_{-1}^* \cdot k_{-2} + (k_{-1}^* + k_2) \cdot k_3} \right) \\ &\cdot \left(\frac{k_1 \cdot S_0 \cdot (k_{-2} + k_3)}{k_{-1}^* \cdot k_{-2} + (k_{-1}^* + k_2) \cdot k_3} \right)^{-1} \\ &= \frac{k_2}{k_{-2} + k_3} = Q \end{aligned} \quad (25)$$

The most right side of Eq. 25 is identical to that of Eq. 11, showing that assuming reversibility of the sterol import step does not affect the steady state sterol distribution in the PM. This is an important result with the consequence that the whole thermodynamic flux analysis presented above remains valid also for reversible and ATP-dependent sterol import by Aus1/Pdr11. In contrast to the irreversible sterol import (Eq. 1), flux control is now shared between the forward and backward step in the first transport step (not shown). Note that the relations above, i.e. expressions relating the flux J (i.e., ν_1) to the chemical potential differences, those quantifying sterol abundance in each leaflet at steady state (Eqs. 3a, 3b, 11, 17 and 24a, 24b) and the steady state transbilayer sterol distribution in the PM (Eq. 25) are generally valid for linear import kinetics. In the following, we will only use ν_1 for the Aus1/Pdr11-catalyzed sterol import step, irrespective of $\nu_1 = k_1 \cdot S_0$ (low-substrate regime, a), above) or $\nu_1 = \nu_{\max}$ (high-substrate regime, b), above).

Model of sterol transport in yeast with two sterol pools in each PM leaflet

Linearized model of sterol complex formation in the PM only

The model analysis so far predicts that passive sterol redistribution to the inner leaflet (i.e., preferred inward flipping, $q_2 > 0$) is the main driving force for the observed sterol asymmetry in the PM with little counterbalance from active transport. In the following, a mechanism is discussed by which sterol can be enriched in one leaflet without invoking differing flip and flop rates for passive sterol exchange between the leaflets. It has been suggested that the PM of eukaryotic cells is sub-compartmentalized into an active sterol pool, which rapidly responds to changes in lipid composition or sterol abundance, and a ‘passive’ pool, which is restraint to the PM by complex formation with phospholipids [15, 50]. The molecular mechanisms of sterol sequestration in the complexed ‘inactive’ pool are not clear at the moment, but could involve preferred interaction with some lipid species, like sphingolipids, or with membrane-embedded or -associated proteins [14, 50, 51]. The ‘active’

pool in each leaflet is meant as being freely available for exchange including complex formation and flip-flop to the opposite leaflet. Its definition is routed in a thorough thermodynamic analysis of phospholipid-cholesterol phase diagrams in lipid model systems, in which a steep increase in cholesterol’s chemical activity, a , with $a = \exp(\mu/k_B \cdot T)$ at critical cholesterol mole fractions was found [15, 52]. The chemical activity surmises all molecular interactions of sterol in the bilayer defining its available volume as function of sterol concentration [52, 53]. Due to their concentration-dependent lipid condensing effects, higher sterols like cholesterol ergosterol impact the available volume in the bilayer which in turn affects sterol-phospholipid interactions. Several physico-chemical models have been put forward to explain the highly non-linear dependence of cholesterol’s chemical potential in membranes on bilayer sterol mole fraction, as recently reviewed [8]. To keep our analysis simple and transparent, we employ a model based on mass-action kinetics involving sterol-phospholipid complexes [15, 52, 53]. This approach also has another advantage, namely that the sterol binding partner potentially can be other types of molecules, like membrane proteins. To include a complexed sterol pool in our analysis, the irreversible import model was extended to.



Now, we define the active or free sterol in the outer PM leaflet as S_1 and the active sterol in the inner PM leaflet as S_2 . In both leaflets, n molecules of free sterol can bind to m molecules of phospholipids, designated as P_1 for the outer and P_2 for the inner leaflet, respectively. Such binding results in formation of complexes named C_1 for the outer and C_2 for the inner leaflet, respectively. This is justified by the observation, that condensed complexes can form between sterols and sphingolipids, as primarily found in the outer PM leaflet, but also with PS, being enriched in the cytoplasmic PM leaflet [15, 52, 54]. Condensed complexes are supposed to cover less membrane area than the sum of the contributing constituents would in the non-complexed state, thereby accounting for cholesterol’s condensing effect on lipid membranes [53, 55]. The free or active sterol can move between the leaflets and across the bilayer with rate ν_2 in our model, which ensures that free and complexed pools in each leaflet are kinetically coupled. That is, free sterol in the outer leaflet, S_1 , flipped to the inner can be replenished by dissociation of the condensed complex in the outer leaflet (with rate ν_4). Similarly, active sterol released into the cytoplasm from the inner

leaflet (with rate v_3) can be replenished from both complexed sterol pools; from dissociation of the condensed complex in the inner leaflet (with rate v_5) and from dissociation of the condensed complex in the outer leaflet (with rate v_4) followed by flip of the liberated free sterol from the outer to the inner leaflet (with rate v_2). For simplicity, we consider only 1st order complex formation setting $n = m = 1$ as previously suggested for ternary lipid mixtures in model membrane vesicles [56]. Further, we assume for the moment the phospholipids to be in excess for the binding such that we obtain pseudo first order rate constants for binding in the outer leaflet, $k_4 = k_4^* \cdot P_1$ and in the inner leaflet, $k_5 = k_5^* \cdot P_2$. This implies that sterol inserted into the PM from extracellular sources to be a minor component, such that complex formation does not consume the sterol binding partners. This constrain is now set for simplicity and transparency of the analysis but will later be removed (see below). Together, this gives the following transport rates: $v_1 = \text{const.}$, $v_2 = k_2 \cdot S_1 - k_{-2} \cdot S_2$, $v_3 = k_3 \cdot S_2$, $v_4 = k_4 \cdot S_1 - k_{-4} \cdot C_1$ and $v_5 = k_5 \cdot S_2 - k_{-5} \cdot C_2$. The resulting ODE system reads:

$$\begin{aligned} \frac{dS_1}{dt} &= v_1 - v_2 - v_4 = k_1 \cdot S_0 - (k_2 + k_4) \cdot S_1 + k_{-2} \cdot S_2 + k_{-4} \cdot C_1 \\ \frac{dS_2}{dt} &= v_2 - v_3 - v_5 = k_2 \cdot S_1 - (k_{-2} + k_3 + k_5) \cdot S_2 + k_{-5} \cdot C_2 \\ \frac{dC_1}{dt} &= v_4 = k_4 \cdot S_1 - k_{-4} \cdot C_1 \\ \frac{dC_2}{dt} &= v_5 = k_5 \cdot S_2 - k_{-5} \cdot C_2 \end{aligned} \tag{27a - d}$$

The steady state amount of active sterol in the outer and inner leaflet of the PM is:

$$\overline{S_1} = \frac{k_1 \cdot S_0 \cdot (k_{-2} + k_3)}{k_2 \cdot k_3} = \frac{v_1 \cdot (k_{-2} + k_3)}{k_2 \cdot k_3} \tag{28a}$$

$$\overline{S_2} = \frac{k_1 \cdot k_2 \cdot S_0}{k_2 \cdot k_3} = \frac{k_1 \cdot S_0}{k_3} = \frac{v_1}{k_3} \tag{28b}$$

This is identical to the one-pool irreversible model (Eq. 3a and 3b), showing that active sterol moves freely between the two PM leaflets. That does not mean, though, that the complexed sterol pools in each leaflet are independent of each other. In fact, it can be easily seen from the steady state solutions for the sterol in complexes, that:

$$\begin{aligned} \overline{C_1} &= \frac{k_4 \cdot v_1 \cdot (k_{-2} + k_3)}{k_2 \cdot k_3 \cdot k_{-4}} = \frac{q_4 \cdot v_1 \cdot (k_{-2} + k_3)}{k_2 \cdot k_3} \\ &= q_4 \cdot \overline{S_1} \end{aligned} \tag{29a}$$

$$\overline{C_2} = \frac{k_5 \cdot v_1}{k_{-5} \cdot k_3} = \frac{q_5 \cdot v_1}{k_3} = q_5 \cdot \overline{S_2} \tag{29b}$$

Here, the equilibrium constants for complex formation in the outer and inner leaflet are $q_4 = k_4/k_{-4}$ and $q_5 = k_5/k_{-5}$, respectively. Using Eqs. 28a and 28b in 29a, one finds that sterol complex in the outer leaflet at steady state can be expressed as function of free sterol in the inner leaflet as

$$\overline{C_1} = \frac{q_4 \cdot \overline{S_2} \cdot (k_{-2} + k_3)}{k_2} \tag{29c}$$

Similar relations can be found to express sterol complex in the inner leaflet at steady state as function of free sterol in the outer leaflet (not shown), clearly establishing that all four sterol pools in the PM are connected with each other. The total amount of sterol in the outer leaflet, S_T^o , and in the inner leaflet, S_T^i , becomes:

$$\begin{aligned} S_T^o &= \overline{S_1} + \overline{C_1} = (1 + q_4) \cdot \overline{S_1} \\ S_T^i &= \overline{S_2} + \overline{C_2} = (1 + q_5) \cdot \overline{S_2} \end{aligned} \tag{30a, b}$$

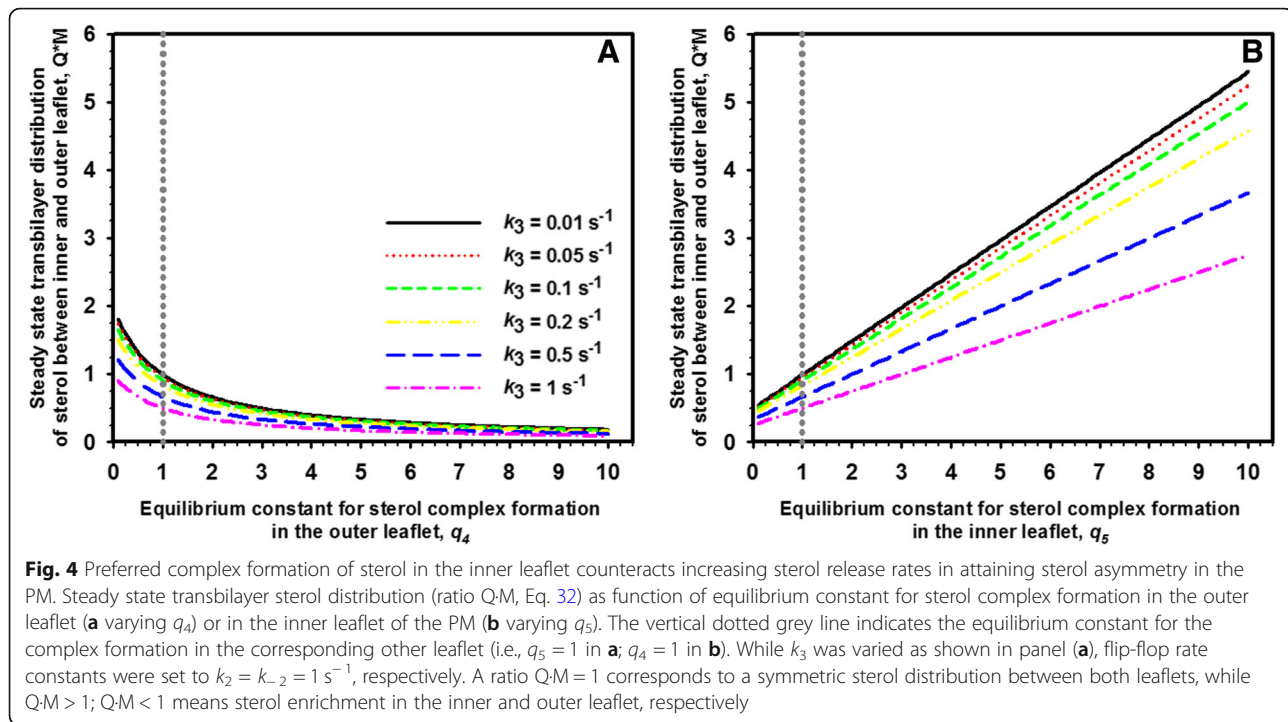
The steady state ratio of sterol between the two PM leaflets reads:

$$\begin{aligned} S_T^i/S_T^o &= (\overline{S_2} + \overline{C_2})/(\overline{S_1} + \overline{C_1}) = \frac{(1 + q_5) \cdot \overline{S_2}}{(1 + q_4) \cdot \overline{S_1}} \\ &= \frac{k_2 \cdot k_{-4} \cdot (k_5 + k_{-5})}{(k_{-2} + k_3) \cdot (k_4 + k_{-4}) \cdot k_{-5}} \end{aligned} \tag{31}$$

This can be simplified to:

$$S_T^i/S_T^o = \frac{k_2}{k_{-2} + k_3} \cdot \frac{(1 + q_5)}{(1 + q_4)} = Q \cdot \frac{(1 + q_5)}{(1 + q_4)} \tag{32}$$

From Eq. 31/32, one can draw two important conclusions; first, the steady state transbilayer sterol distribution is also for the two-pool model independent of sterol influx, v_1 . Second, introducing two sterol pools (free and in complex) into each PM leaflet modifies the original steady state transbilayer sterol distribution, Q , by the factor $M = \frac{(1+q_5)}{(1+q_4)}$. The steady state ratio of sterol between the two PM leaflets as function of the equilibrium constants for complex formation in either leaflet is shown Fig. 4. Here, the equilibrium constant not being varied is set equal to 1 (i.e. $q_5 = 1$ in Fig. 4a and $q_4 = 1$ in Fig. 4b; dotted grey line), meaning that half of total leaflet sterol is in complexes and half is free in either case. The equilibrium constant for passive sterol flip-flop, q_2 , is also set to one, meaning that active sterol does not show any preference for either leaflet in this model. More sterol in complexes in the outer leaflet, i.e., less being free or ‘active’ lowers the total amount of sterol in the inner side of the PM in a non-linear manner (Fig. 4a). If complex formation



takes place primarily in the inner leaflet, the steady state ratio of sterol is shifted to this side of the bilayer (Fig. 4b). Thus, despite identical passive flip-flop rates, sterol asymmetry can be controlled in this model by differing interaction of sterol with phospholipids in either leaflet. As before for the one-pool model, increasing non-vesicular sterol outflux described by rate constant k_3 lowers the attainable steady state sterol ratio between both PM leaflets. One also sees that sterol enrichment in the inner leaflet on expense of the outer is only possible if complex formation takes place preferentially with phospholipids in the inner PM leaflet (i.e., we must have $q_5 \gg q_4$). Interestingly ergosterol seems to be excluded from gel-like domains formed by outer-leaflet sphingolipids in the yeast PM [57]. This could effectively lower complex formation in the outer PM leaflet (i.e., q_4). In addition, sterols might be drawn to the inner half of the PM to reduce spontaneous bilayer curvature caused by the inverted cone shape of PE species and by charge repulsion of PS in the inner leaflet [45, 58]. Both processes could transiently immobilize some sterol in complexes, thereby raising q_5 and stabilizing sterol asymmetry in the yeast PM. Alternatively, ergosterol might not at all be in complex with phospholipids in the inner leaflet but rather bind to cytoplasmic proteins accessing sterol from the inner PM leaflet. In fact, peripheral proteins can sequester sterols in the PM. This has been shown for

perfringolysin derivatives bound to the outer PM leaflet which prevented non-vesicular sterol transport to the ER [59, 60]. Accordingly, in our model Eq. 26b, c could also describe formation of protein – sterol complexes which would enrich ergosterol in the inner compared to the outer PM leaflet. Clearly more work is required to determine the underlying molecular mechanisms of sterol sequestration.

For the 2-pool model, the steady state sterol fluxes across the PM read:

$$\begin{aligned} \bar{v}_2 &= \bar{v}_3 = v_1 \\ \bar{v}_4 &= \bar{v}_5 = 0 \end{aligned} \quad (33)$$

That is, like in the irreversible one-pool model, only one flux exists at steady state, which is entirely set by the sterol import rate via Aus1/Pdr11, irrespective of whether the system is in the low- or high-substrate regime. Sterol in complexes with leaflet-specific phospholipids or with membrane-attached or –embedded proteins does not contribute to the steady state sterol flux in this model. This is an important conclusion, as it shows that sterol flux between various membrane pools can be fast, even though sterol gradients are stable at steady state.

Finally, we compare the expressions for the total PM associated sterol in case of the irreversible one- and two pool models, respectively. For the one-pool model, we had (see above and Fig. 3a):

$$S_T = \bar{S}_1 + \bar{S}_2 = \frac{v_1 \cdot (k_2 + k_{-2} + k_3)}{k_2 \cdot k_3} \quad (34)$$

With Eqs. 28a, 28b and 30a, b, we get for the two-pool model

$$S_T = \bar{S}_1 + \bar{C}_1 + \bar{S}_2 + \bar{C}_2 = \frac{v_1 \cdot (k_2 \cdot (1 + q_5) + (k_{-2} + k_3) \cdot (1 + q_4))}{k_2 \cdot k_3} \quad (35)$$

By comparing Eqs. 34 and 35, one sees, that the amount of sterol in the PM at steady state will be a linear increasing function for increasing q_4 or q_5 . That is, complex formation in either leaflet retains sterol in the PM. For q_4 and q_5 being zero, we recover the solution for the one pool model, Eq. 34.

Steady state model including two sterol pools in each PM leaflet, transport to the ER and esterification

Linearized model of sterol complex formation in the PM and ER

Cholesterol in mammalian cells and ergosterol in yeast are very abundant in the PM compared to the ER, even though the biochemical machinery for sterol synthesis and esterification reside mostly in the ER, and there is continuous sterol exchange taking place between both compartments [4, 10, 13, 14]. It has been suggested that difference in lipid composition with strongly varying affinity for sterols exist between both organelles which might be responsible for establishment and maintenance of this strong sterol gradient between PM and ER [8, 13, 61]. Thermodynamic equilibrium models have been put forward which assume that sterols in the PM exist in a free or ‘active’ pool and in a pool bound with differing affinity to phospholipids in the PM versus the ER, which could result in identical chemical potentials for sterols in each membrane despite differing concentrations [10, 15, 62]. How a non-equilibrium steady state of sterol influx and esterification would affect such a 2-pool model of sterol in the PM and ER has not been studied. Here, we extend the two-pool model for the PM to include rapid non-vesicular sterol exchange with the ER followed by explicit consideration of sterol esterification in this compartment. The latter allows us to dissect separately the contribution of non-vesicular sterol exchange between PM and ER and sterol esterification. We make again use of the fact, that sterol extraction from membranes by STPs but not diffusion of protein-sterol complexes in the cytoplasm is rate-limiting for sterol exchange between PM and ER, justifying the use of an ODE system to describe the following process:



As before, we have the active or free sterol in the outer PM leaflet as S_1 and the active sterol in the inner PM leaflet as S_2 . In both leaflets, $n = 1$ molecules of free sterol can bind to $m = 1$ molecules of phospholipids, designated as P_1 for the outer and P_2 for the inner leaflet, respectively. Such binding results in formation of complexes named C_1 for the outer and C_2 for the inner leaflet, respectively. Only the free or active sterol can move between the leaflets and across the bilayer. For simplicity, we consider again the phospholipids to be in excess for the binding such that we obtain pseudo first order rate constants for binding in the outer leaflet, $k_4 = k_4^* \cdot P_1$ and in the inner leaflet, $k_5 = k_5^* \cdot P_2$. Exactly the same approach is used to describe sterol complex formation with phospholipids of the ER in Eq. 36b, c, d, where S_3 is the freely moving sterol pool, and C_3 describes the sterol complexes in the ER. In addition, we consider now reversible sterol exchange between PM and ER and assume that forward and backward rate constants for sterol flip flop and for exchange between PM and ER are identical giving $q_2 = q_3 = 1$. Sterol esterification by Are2 is creating an irreversible sink of non-esterified sterol described by rate v_7 . It follows linear kinetics, which can be justified in the low substrate regime using a linearization of the Michaelis-Menten rate law, as described in Eqs. 5 and 6 for the Aus1/Pdr11 membrane transporter (see above). This gives the following transport rates: $v_1 = \text{const.}$, $v_2 = k_2 \cdot (S_1 - S_2)$, $v_3 = k_3 \cdot (S_2 - S_3)$, $v_4 = k_4 \cdot S_1 - k_{-4} \cdot C_1$, $v_5 = k_5 \cdot S_2 - k_{-5} \cdot C_2$, $v_6 = k_6 \cdot S_3 - k_{-6} \cdot C_3$ and $v_7 = k_7 \cdot S_3$. Thus, net sterol transfer from the outer to the inner PM leaflet and from the PM to the ER takes place as long as $v_2, v_3 > 0$, which is ensured as long as $S_1 > S_2 > S_3$. The resulting ODE system reads:

$$\begin{aligned} \frac{dS_1}{dt} &= v_1 - v_2 - v_4 = k_1 \cdot S_0 - (k_2 + k_4) \cdot S_1 + k_2 \cdot S_2 + k_{-4} \cdot C_1 \\ \frac{dS_2}{dt} &= v_2 - v_3 - v_5 = k_2 \cdot S_1 - (k_3 + k_5) \cdot S_2 + k_{-5} \cdot C_2 + k_3 \cdot S_3 \\ \frac{dS_3}{dt} &= v_3 - v_6 - v_7 = k_3 \cdot S_2 - (k_6 + k_7) \cdot S_3 + k_{-6} \cdot C_3 \\ \frac{dC_1}{dt} &= v_4 = k_4 \cdot S_1 - k_{-4} \cdot C_1 \\ \frac{dC_2}{dt} &= v_5 = k_5 \cdot S_2 - k_{-5} \cdot C_2 \\ \frac{dC_3}{dt} &= v_6 = k_6 \cdot S_3 - k_{-6} \cdot C_3 \end{aligned} \quad (37a - f)$$

The steady state amount of active sterol in the outer and inner leaflet of the PM now reads:

$$\bar{S}_1 = v_1 \cdot \left(\frac{1}{k_2} + \frac{1}{k_3} + \frac{1}{k_7} \right) \quad (38)$$

$$\overline{S}_2 = \frac{v_1 \cdot (k_3 + k_7)}{k_3 \cdot k_7} \quad (39)$$

Setting $r = \frac{k_7}{k_3+k_7}$ as a weighted rate constant for sterol esterification, Eqs. 37a-f and 38 read

$$\overline{S}_1 = \frac{v_1 \cdot (k_3 \cdot r + k_2)}{k_2 \cdot k_3 \cdot r} \quad (40)$$

$$\overline{S}_2 = \frac{v_1}{k_3 \cdot r} \quad (41)$$

Thus, the expressions for the amount of free or ‘active’ sterol in the outer and inner PM leaflet at steady state contain now the weighted rate constant for sterol esterification, r . Otherwise, they are equal to the respective expressions for the one-pool irreversible model (Eq. 3b) and the two-pool model without considering the ER explicitly (Eq. 28b), when setting $k_2 = k_{-2}$. When comparing Eqs. 40 and 41, one sees that the steady concentration of free sterol in the outer PM leaflet is always larger than that in the inner PM leaflet (i.e., $\overline{S}_1 > \overline{S}_2$) for positive rate constants, which is in accordance with net transfer of sterol from the outer to the inner PM leaflet followed by net transfer to the ER (i.e., with $v_2, v_3 > 0$). The steady state solutions for the sterol in complexes read:

$$\begin{aligned} \overline{C}_1 &= \frac{q_4 \cdot v_1 \cdot (k_3 \cdot k_7 + k_2 \cdot (k_3 + k_7))}{k_2 \cdot k_3 \cdot k_7} \\ &= \frac{q_4 \cdot v_1 \cdot (k_3 \cdot r + k_2)}{k_2 \cdot k_3 \cdot r} = q_4 \cdot \overline{S}_1 \end{aligned} \quad (42)$$

$$\overline{C}_2 = \frac{q_5 \cdot (k_3 + k_7) \cdot v_1}{k_3 \cdot k_7} = \frac{q_5 \cdot v_1}{k_3 \cdot r} = q_5 \cdot \overline{S}_2 \quad (43)$$

$$\overline{C}_3 = \frac{k_6 \cdot v_1}{k_7 \cdot k_{-6}} = q_6 \cdot \overline{S}_3 \quad (44)$$

Thus, the relation between complex and free sterol, as found for the 2-pool PM model, is maintained (compare to Eq. 29a, 29b, 29c), and the same relation holds between free and bound sterol in the ER. Thus, not only non-vesicular sterol exchange dynamics but also the kinetics of sterol esterification affects sterol abundance in PM and the ER in this extended model. The latter prediction is in line with experimental observations in which non-vesicular transport of DHE from the PM to the ER, its esterification and storage in lipid droplets was found to require ATP and Are2 activity [27]. The puzzling observation that ATP-depletion inhibited non-vesicular sterol transport from the PM can be understood in light of our findings; sterol esterification requires sterols and activated fatty acids, and the activation of fatty acids with coenzyme A consumes ATP. Despite

the fact that we model this complex process by a single irreversible step, any change of Are2 activity or ATP-dependent provision of its substrate should translate into a change of rate constant k_7 . The steady state ratio of sterol between the two PM leaflets now reads:

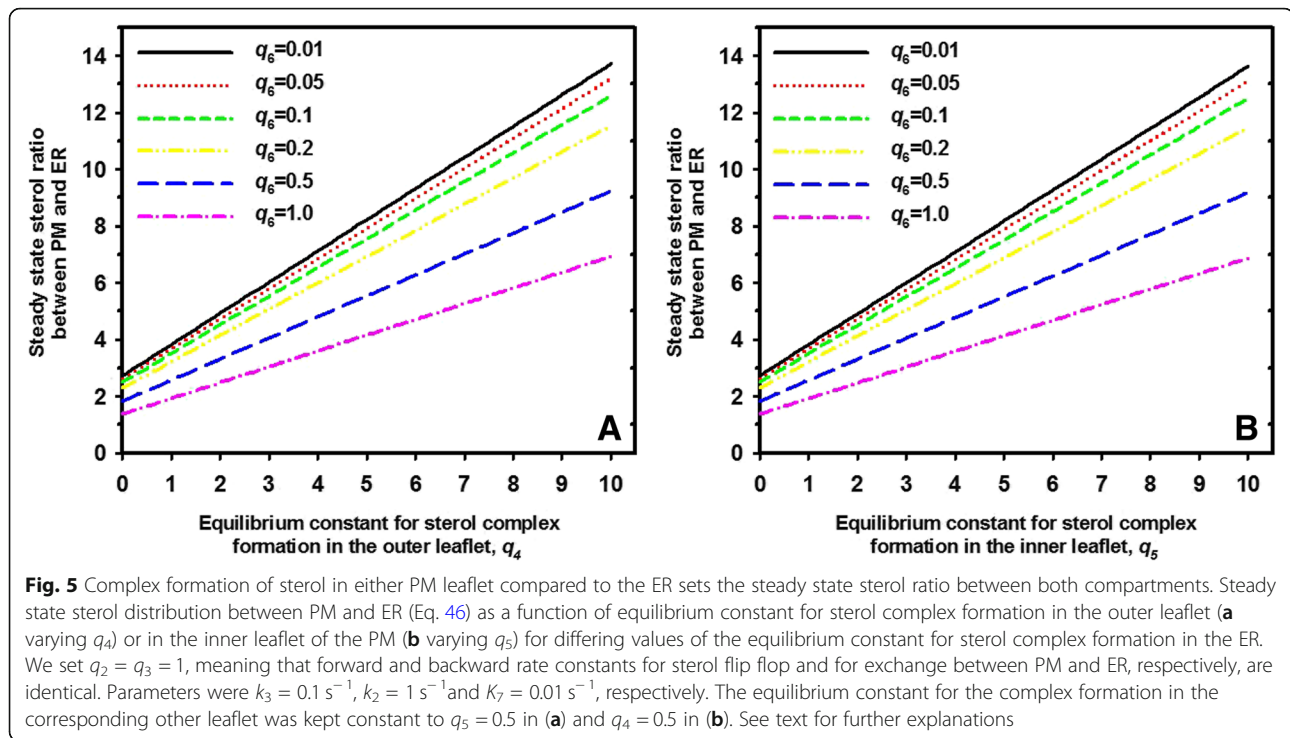
$$\begin{aligned} S_T^i/S_T^o &= (\overline{S}_2 + \overline{C}_2)/(\overline{S}_1 + \overline{C}_1) \\ &= \frac{k_2}{(k_2 + k_3 \cdot r)} \cdot \frac{(1 + q_5)}{(1 + q_4)} = Q' \cdot \frac{(1 + q_5)}{(1 + q_4)} \end{aligned} \quad (45)$$

Thus, the expression looks very similar to the one for the 2-pool PM model when setting $k_2 = k_{-2}$. (Eqs. 31 and 32). The only difference is the appearance of $r = \frac{k_7}{k_3+k_7}$. This weighted rate constant for sterol esterification must be smaller than 1 as long as $k_3, k_7 > 0$. This situation will prevail in most experimental settings, and Eq. 44 show that the kinetics of sterol esterification in the ER can impact the sterol transbilayer distribution in the PM at steady state. When comparing Eq. 45 with 40 and 41, above, one sees that $\overline{S}_1 = \overline{S}_2/Q'$, and as $Q' < 1$, always, the free sterol pool in the outer leaflet is always larger than that in the inner PM leaflet. An important conclusion from this analysis is that net enrichment of sterol in the inner PM leaflet can only be achieved, if $(1 + q_5)/(1 + q_4) >> 1$, i.e., when the sterol complexing capacity of the inner leaflet significantly exceeds that of the outer PM leaflet.

Finally, we ask, what is the steady state sterol distribution between PM and ER and how is it affected by the various transport steps. By setting PM_T and ER_T the total sterol amount in the PM and ER at steady state, we find:

$$\begin{aligned} \frac{PM_T}{ER_T} &= \frac{\overline{S}_1 + \overline{C}_1 + \overline{S}_2 + \overline{C}_2}{\overline{S}_3 + \overline{C}_3} \\ &= \frac{k_3 \cdot k_7 \cdot (1 + q_4) + k_2 \cdot (k_3 + k_7) \cdot (2 + q_4 + q_5)}{k_2 \cdot k_3 \cdot (1 + q_6)} \end{aligned} \quad (46)$$

When plotting this ratio as function of the equilibrium constants for complex formation in the outer or inner PM leaflet, one can determine how complex formation affects sterol partitioning between both organelles at steady state (Fig. 5). As the ER contains mostly unsaturated phospholipids with low propensity to pair with cholesterol, the equilibrium constant for sterol complex formation in the ER, q_6 , is set to be low i.e. between $q_6 = 0.1$ and $q_6 = 1$. The analysis shows, that preferred sterol complex formation in either the outer or inner PM leaflet result in sterol accumulation in the PM compared to the ER. If the ability of the ER to bind sterol is increased, an even



higher complex formation must be ensured in the PM to maintain the steady state sterol distribution between both organelles. For example, for a ratio of $80:20 = 4$ between PM and ER, one would need for the equilibrium constant of sterol complex formation in the outer leaflet $q_4 = 1.2$ and in the inner leaflet $q_5 = 0.5$ for complex formation in the ER with $q_6 = 0.01$ (straight black line in Fig. 5a). The same steady state ratio can be obtained if complex formation dominates in the inner PM leaflet ($q_4 = 0.5$; $q_5 = 1.2$ for $q_6 = 0.01$; straight black line in Fig. 5b). However, if the complex formation is stronger in the ER, e.g., $q_6 = 1$, one would need a much stronger sterol complex formation in either the outer or inner PM leaflet (e.g. $q_4 = 4.8$; Fig. 5a, pink dashed-dotted line). Thus, the model presented here quantifies the known steady state sterol gradient between PM and ER based on differing sterol membrane interactions in each organelle.

Bimolecular sterol complex formation in the PM and ER

The above model made the simplifying assumption, that phospholipids are in excess for the binding such that we obtained pseudo first order rate constants for binding in the outer leaflet, $k_4 = k_4^* \cdot P_1$, in the inner leaflet, $k_5 = k_5^* \cdot P_2$ and in the ER, $k_6 = k_6^* \cdot P_3$. This assumption is only valid under certain assumptions; namely that all phospholipid can form complexes with sterols, and that the mole fraction of sterols in each membrane is low. The latter assumption only holds for relatively large

cytoplasmic release combined with low abundance of ergosterol in the medium and/or low transport activity of Aus/Pdr11, both resulting in low import fluxes, v_1 . The foregoing assumption only applies to cases, where all phospholipids in a membrane would interact equally with sterols, which is likely not realistic for a cellular membrane. Instead, membrane lipids bearing saturated acyl chains would interact preferentially (i.e., would form condensed complexes with ergosterol or cholesterol), while unsaturated phospholipids might avoid direct contact to sterols [53, 55]. A more realistic scenario is to consider complex formation explicitly, which requires solving the steady state system for a bimolecular complexation rate in each membrane pool. This gives the following transport rates: $v_1 = \text{const.}$, $v_2 = k_2 \cdot (S_1 - S_2)$, $v_3 = k_3 \cdot (S_2 - S_3)$, $v_4 = k_4 \cdot S_1 \cdot P_1 - k_{-4} \cdot C_1$, $v_5 = k_5 \cdot S_2 \cdot P_2 - k_{-5} \cdot C_2$, $v_6 = k_6 \cdot S_3 \cdot P_3 - k_{-6} \cdot C_3$ and $v_7 = k_7 \cdot S_3$. Here, P_1 , P_2 and P_3 are the sterol binding partners for complex formation in each pool, assumed to be saturated phospholipids for simplicity. A stoichiometry of 1:1, sterol:phospholipid is chosen to simplify the analysis and as justified by studies on model membranes of certain lipid compositions [55, 63]. This bi-molecular model can account for high sterol mole fraction and also for limiting availability of phospholipid binding partners, a key ingredient of the condensed complex model. In fact, condensed complexes have been invoked to explain the phase behavior of binary sterol-phospholipid complexes but also of ternary mixtures of sterol, unsaturated and saturated phospholipids,

in which only the latter are assumed to interact preferentially (be ‘reactive’ according to [53, 55]). With this extension the resulting ODE for our steady state system reads:

$$\begin{aligned}
 \frac{dS_1}{dt} &= v_1 - v_2 - v_4 = k_1 \cdot S_0 - (k_2 + k_4 \cdot P_1) \cdot S_1 + k_2 \cdot S_2 + k_{-4} \cdot C_1 \\
 \frac{dS_2}{dt} &= v_2 - v_3 - v_5 = k_2 \cdot S_1 - (k_2 + k_3 + k_5 \cdot P_2) \cdot S_2 + k_{-5} \cdot C_2 + k_3 \cdot S_3 \\
 \frac{dS_3}{dt} &= v_3 - v_6 - v_7 = k_3 \cdot S_2 - (k_3 + k_6 \cdot P_3 + k_7) \cdot S_3 + k_{-6} \cdot C_3 \\
 \frac{dC_1}{dt} &= v_4 = k_4 \cdot S_1 \cdot P_1 - k_{-4} \cdot C_1 \\
 \frac{dC_2}{dt} &= v_5 = k_5 \cdot S_2 \cdot P_2 - k_{-5} \cdot C_2 \\
 \frac{dC_3}{dt} &= v_6 = k_6 \cdot S_3 \cdot P_3 - k_{-6} \cdot C_3 \\
 \frac{dP_1}{dt} &= -v_4 = -k_4 \cdot S_1 \cdot P_1 + k_{-4} \cdot C_1 \\
 \frac{dP_2}{dt} &= -v_5 = -k_5 \cdot S_2 \cdot P_2 + k_{-5} \cdot C_2 \\
 \frac{dP_3}{dt} &= -v_6 = -k_6 \cdot S_3 \cdot P_3 + k_{-6} \cdot C_3
 \end{aligned}
 \tag{47a - i}$$

At first glance, this system consisting of nine coupled ODEs looks rather complicated and apparently tedious to solve, but it simplifies considerably for the steady state scenario; since concentrations do not change at steady state, all expressions are set to zero. This implies $v_4 = v_5 = v_6 = 0$, such that the steady state concentration of active sterol in the PM and ER can be calculated from the much simpler system, where we get for the outer and inner leaflet of the PM again:

$$\overline{S_1} = v_1 \cdot \left(\frac{1}{k_2} + \frac{1}{k_3} + \frac{1}{k_7} \right)
 \tag{48}$$

$$\overline{S_2} = \frac{v_1 \cdot (k_3 + k_7)}{k_3 \cdot k_7}
 \tag{49}$$

This is identical to the expressions derived for the linearized model (Eqs. 38 and 39, above), showing that bimolecular complex formation of sterol in each leaflet does not affect the steady state concentrations of active sterol. The steady state amount of active sterol in the ER is also identical to the linear model and reads:

$$\overline{S_3} = \frac{v_1}{k_7}
 \tag{50}$$

One also sees that the system has only one non-vanishing steady state flux, which is again $v_1 = v_2 = v_3 = v_7$. This is an important and somehow surprising result; flux of active sterol through the Aus1/Pdr11 importers, flip-flop across the PM, transport to the ER and esterification become equal at steady state, while the complexed sterol pools in each membrane do not explicitly contribute to this flux. So, how are sterol complexes related to active sterol at steady state?

Complexes of sterol and phospholipid give rise to non-linear sterol pool sizes in the PM and ER

To derive this we make use of a conservation relation, which is that the concentration of phospholipid in the unbound form and in complexes is preserved in each pool. That means, the total pool of sterol binding partners in the outer leaflet (P_{T1}), in the inner leaflet (P_{T2}) and in the ER (P_{T3}) is constant, such that.

$$\overline{C_i} + \overline{P_i} = P_{Ti}, \quad \forall \quad i = 1, 2, 3
 \tag{51}$$

With that used in Eq. 47a-i e, f, one can derive the steady state concentrations of sterol in complexes as

$$\begin{aligned}
 \overline{C_1} &= \frac{q_4 \cdot \overline{S_1} \cdot P_{T1}}{k_4 \cdot \overline{S_1} + k_{-4}} = \frac{v_1 \cdot k_4 \cdot P_{T1} \cdot (k_3 \cdot k_7 + k_2 \cdot (k_3 + k_7))}{v_1 \cdot k_3 \cdot k_4 \cdot k_7 + k_2 \cdot (k_3 \cdot k_7 \cdot k_{-4} + v_1 \cdot k_4 \cdot (k_3 + k_7))} \\
 &= \frac{v_1 \cdot q_4 \cdot P_{T1} \cdot (k_3 \cdot r + k_2)}{v_1 \cdot q_4 \cdot (k_3 \cdot r + 1) + k_2 \cdot k_3 \cdot r}
 \end{aligned}
 \tag{52}$$

$$\begin{aligned}
 \overline{C_2} &= \frac{q_5 \cdot \overline{S_2} \cdot P_{T2}}{k_5 \cdot \overline{S_2} + k_{-5}} \\
 &= \frac{v_1 \cdot k_5 \cdot P_{T2} \cdot (k_3 + k_7)}{k_3 \cdot k_{-5} \cdot k_7 + v_1 \cdot k_5 \cdot (k_3 + k_7)} \\
 &= \frac{v_1 \cdot q_5 \cdot P_{T2}}{k_3 \cdot r + v_1 \cdot q_5}
 \end{aligned}
 \tag{53}$$

$$\begin{aligned}
 \overline{C_3} &= \frac{q_6 \cdot \overline{S_3} \cdot P_{T3}}{k_6 \cdot \overline{S_3} + k_{-6}} = \frac{v_1 \cdot k_6 \cdot P_{T3}}{k_{-6} \cdot k_7 + v_1 \cdot k_6} \\
 &= \frac{v_1 \cdot q_6 \cdot P_{T3}}{k_7 + v_1 \cdot q_6}
 \end{aligned}
 \tag{54}$$

Similar expressions hold for the steady state concentration of non-complexed phospholipid in each pool (not shown). One sees from Eqs. 48 to 50 and the right-hand side of Eqs. 52 to 54 that sterol abundance in each membrane pool is independent of the kinetic rate constants for sterol complex formation and only depends on their ratio, i.e., the respective equilibrium constants q_4 , q_5 and q_6 . Thus, the exact kinetics of sterol complex formation does not impact the sterol pool sizes at steady state. To use this result for simulating the DHE uptake experiments (see above and [31]), we consider the high substrate regime and set $v_1^{MM} = v_{max}$ in a range covering a large range of transporter expression and activity including the calculated value of $v_1^{MM} = 0.033 \text{ nmol}/(\text{l}\cdot\text{s})$, i.e. we set $v_1 = 0.0005\text{--}0.1 \text{ nmol}/(\text{l}\cdot\text{s})$. Sterol binding partners are set to $P_{T1} = 300 \text{ nmol}/\text{l}$ in the outer PM leaflet, $P_{T2} = 1000 \text{ nmol}/\text{l}$ in the cytoplasmic half of the PM and $P_{T3} = 600 \text{ nmol}/\text{l}$. This is only a fraction of total phospholipid in each pool, which, in case of the PM, surmounts for example to around 1300 nmol/l in each PM leaflet [20, 31]. Thus, we assume that the remaining membrane lipids do not contribute to complex formation and are considered as ‘unreactive’ phospholipids, following the nomenclature of [55]. The equilibrium constant for complex formation in the outer PM leaflet is varied

between $q_4 = 0.2$ to 3.0 , while that for the inner leaflet is set to $q_5 = 1.0$ (Fig. 6). These values compare favorably to those used in simulation of condensed complexes in model lipid systems (i.e. two-phase coexistence and rapid release of sterol from lipid monolayers have been observed for equilibrium constants of sterol complexes in the range of $K = 0.5\text{--}2.0$ [15, 52, 53]. However, it has to be noted that the latter parameters were defined based on experiments in lipid monolayers, in which the equilibrium constant for complex formation is a function of surface pressure, something not considered in our model [53].

One sees, that the abundance of imported sterol in the PM (Fig. 6a), the ER (Fig. 6b) and the whole cells (Fig. 6a) depend for low fluxes in a hyperbolic fashion and for higher fluxes in a linear fashion on the sterol influx, ν_1 . For higher propensity to form complexes (here varied for the outer PM leaflet, q_4), the initial rise in uptake (i.e. for low flux values) is larger than for small q_4 . For larger flux values, i.e., above ca. $\nu_1 = 0.5$ nmol/(l·s), these differences vanish, as exemplified for PM and total sterol (Fig. 6a and c). To analyze this further the abundance of

free and complexed sterol as function of sterol influx was plotted separately, here for the ER pool (Fig. 6b). While sterol complexes depend hyperbolically on ν_1 , the active sterol pool depends linearly on sterol influx (compare red, \overline{C}_3 , and black curve, \overline{S}_3 , in Fig. 6b and see Eq. 54 and 50, above). Thus, being the sum of the respective active and complexed sterol pools, total sterol in each compartment becomes a combination of a hyperbolic and a linear function of sterol influx, ν_1 . A straightforward experimental test of this prediction would be to determine steady state levels of the fluorescent ergosterol analog DHE in the PM and the ER of $\Delta hem1$ yeast cells for varying expression levels of Aus1/Pdr11. In fact, expression of these transporters is under control of the transcription factor Upc2, which in turn senses intracellular sterol abundance [64]. Upc2 was shown to bind ergosterol and DHE and to move to the nucleus to initiate transcription upon sterol depletion [65]. Thus, transcriptional regulation of sterol influx, ν_1 , is likely an important control strategy used by yeast cells under anaerobic growth conditions.

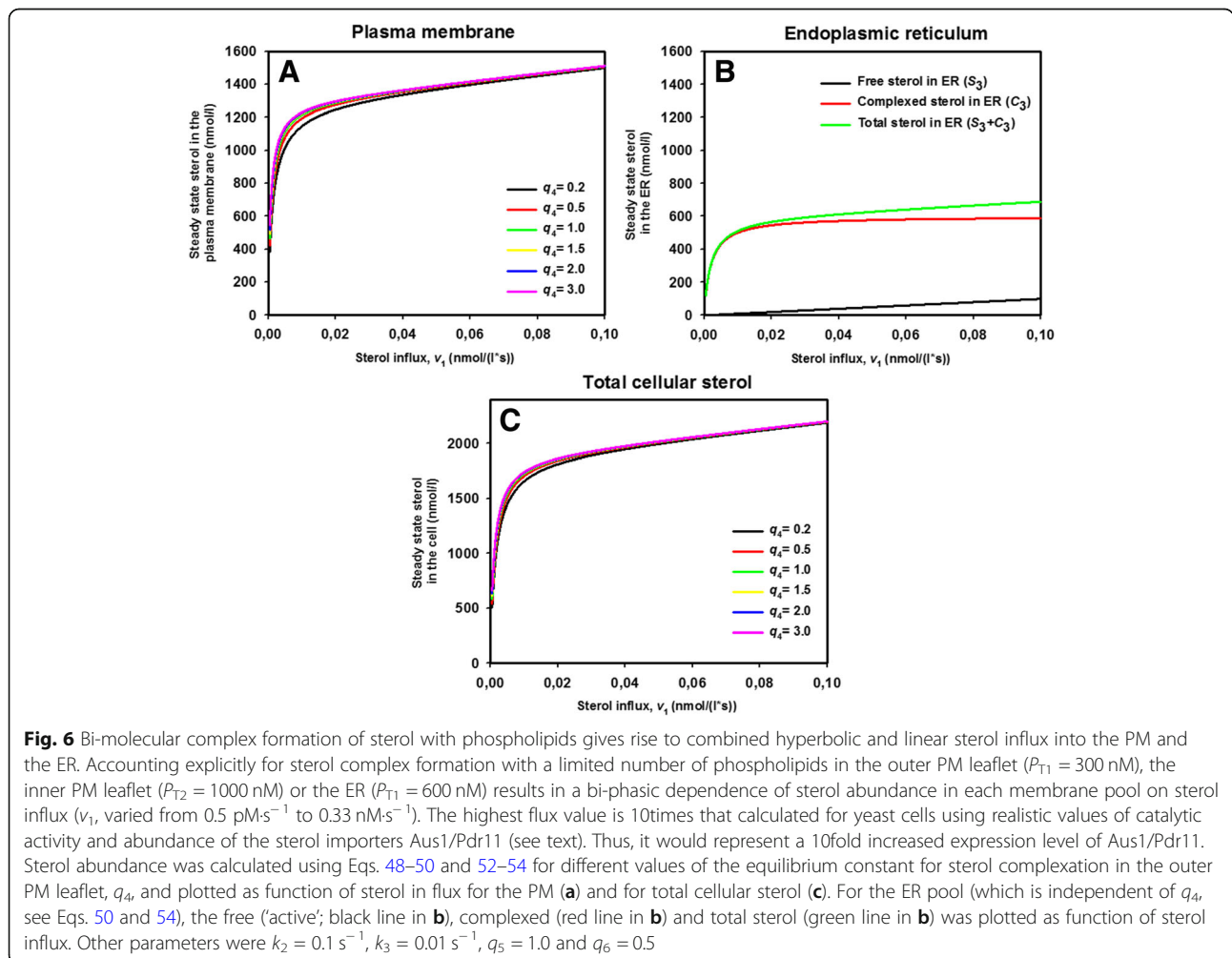


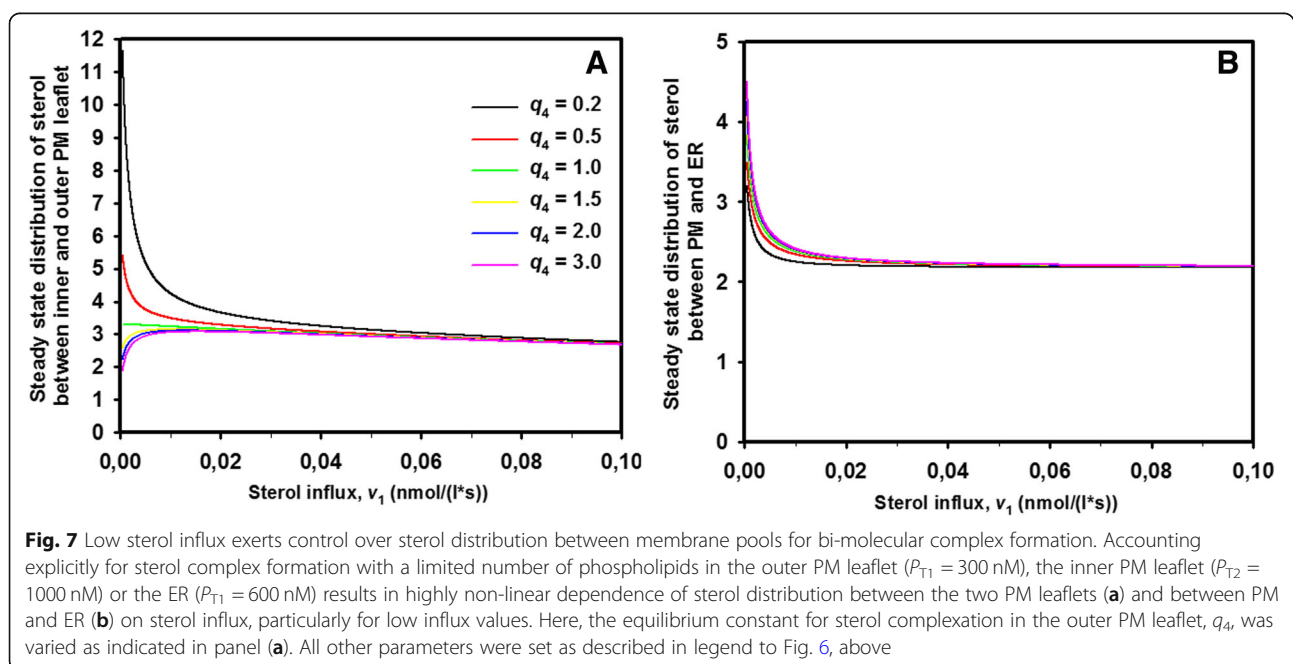
Fig. 6 Bi-molecular complex formation of sterol with phospholipids gives rise to combined hyperbolic and linear sterol influx into the PM and the ER. Accounting explicitly for sterol complex formation with a limited number of phospholipids in the outer PM leaflet ($P_{T1} = 300$ nM), the inner PM leaflet ($P_{T2} = 1000$ nM) or the ER ($P_{T1} = 600$ nM) results in a bi-phasic dependence of sterol abundance in each membrane pool on sterol influx (ν_1 , varied from $0.5 \text{ pM}\cdot\text{s}^{-1}$ to $0.33 \text{ nM}\cdot\text{s}^{-1}$). The highest flux value is 10times that calculated for yeast cells using realistic values of catalytic activity and abundance of the sterol importers Aus1/Pdr11 (see text). Thus, it would represent a 10fold increased expression level of Aus1/Pdr11. Sterol abundance was calculated using Eqs. 48–50 and 52–54 for different values of the equilibrium constant for sterol complexation in the outer PM leaflet, q_4 , and plotted as function of sterol in flux for the PM (a) and for total cellular sterol (c). For the ER pool (which is independent of q_4 , see Eqs. 50 and 54), the free (‘active’; black line in b), complexed (red line in b) and total sterol (green line in b) was plotted as function of sterol influx. Other parameters were $k_2 = 0.1 \text{ s}^{-1}$, $k_3 = 0.01 \text{ s}^{-1}$, $q_5 = 1.0$ and $q_6 = 0.5$

Complexes of sterol and phospholipid can control sterol distribution in the PM and between PM and ER

In previous sections, we showed that the steady state transbilayer distribution of sterol between the two PM leaflets is independent of sterol influx, in yeast mediated by Aus1/Pdr11. Does this also hold true for the non-linear model including sterol complex formation? Sterol distribution between the two PM leaflets can be calculated from Eqs. 48–50 and 52–54, respectively, showing that it depends non-linearly on ν_1 for small influx values (Fig. 7a). Our model predicts that the extent of sterol import into cells directly affects the transbilayer sterol distribution as long as sterol influx is low compared to the ability of complex formation in each leaflet. For larger flux values (i.e., $\nu_1 \geq 0.5 \text{ nmol}/(\text{l}\cdot\text{s})$), sterol distribution between the PM leaflets becomes largely independent of sterol influx and of the sterol complex forming capability of each leaflet (in Fig. 7a shown for varying q_4). Instead the plateau sterol ratio in the PM is primarily set by the abundance of binding partners, e.g. saturated phospholipids in the outer and inner PM leaflet. Thus, our model predicts that preferred location of sterol binding partners in the inner PM leaflet is instrumental for steady state sterol enrichment in this leaflet. To recapitulate the experimentally observed sterol asymmetry of about 80:20 in favor of the inner leaflet, we set phospholipid binding partners in the outer and inner leaflet to $P_1 = 300 \text{ nmol}/\text{l}$ and $P_2 = 1 \mu\text{mol}/\text{l}$, respectively (Fig. 7a). This corresponds to about 20 and 67% of all phospholipids in the outer and inner PM leaflet, respectively. Even though condensed complexes have been shown to form between sterol and outer leaflet lipids,

like sphingolipids as well as inner leaflet lipids, like PS [15, 53], it is currently not supported by experiments, that the inner PM leaflet contains significantly more sterol-interacting lipid species compared to the outer leaflet. One can assume that additional factors, like sterol-binding proteins cause net enrichment of sterol in the cytoplasmic leaflet. Further experimental studies are required to identify and characterize such factors in living cells.

Our model can also recapitulate the experimentally observed 70:30 distribution of ergosterol or DHE between PM and ER for reasonable sterol influx (Fig. 7b). In addition, the model predicts low steady state sterol influx ($\nu_1 \leq 0.01 \text{ nmol}\cdot\text{l}^{-1}\cdot\text{s}^{-1}$) causes a strong dependency of the ability to form sterol complexes in the ER relative to that in the PM on the steady state distribution of sterol between both compartments. Here, the equilibrium constant for sterol complex formation in the outer PM leaflet, q_4 , was varied relative to that in the ER, q_6 , Fig. 7b, but the same qualitative result is obtained by varying q_5 , the equilibrium constants for sterol complexes in the inner PM leaflet (not shown). For larger sterol influx, ($\nu_1 \geq 0.05 \text{ nmol}\cdot\text{l}^{-1}\cdot\text{s}^{-1}$), the steady state sterol ratio between PM and ER becomes completely independent of any sterol complex formation propensity (Fig. 7b). This is, because the active but not the complexed sterol pool moves freely and contributes to the steady state flux between both organelles. As a direct consequence of this result one can predict, that the expression levels of Aus1/Pdr11 in the PM and of Are2 in the ER exert coordinated control over the steady state ratio of sterol between both organelles as long as their



activity does not exceed the sterol complexing capability of the PM. This outcome of our model is in line with some recent results regarding the role played by Aus1/Pdr11 in yeast sterol transport, in which a direct effect of Aus1/Pdr11 activity not only on uptake but also on sterol esterification in the ER has been reported [21, 66]. In one of these studies, even a physical interaction between Aus1/Pdr11 and Are2 at close PM-ER membrane appositions has been suggested [66]. Such an interaction could facilitate the coordination of sterol uptake and esterification via allosteric mechanisms, thereby fine tuning metabolic control of sterol homeostasis in yeast.

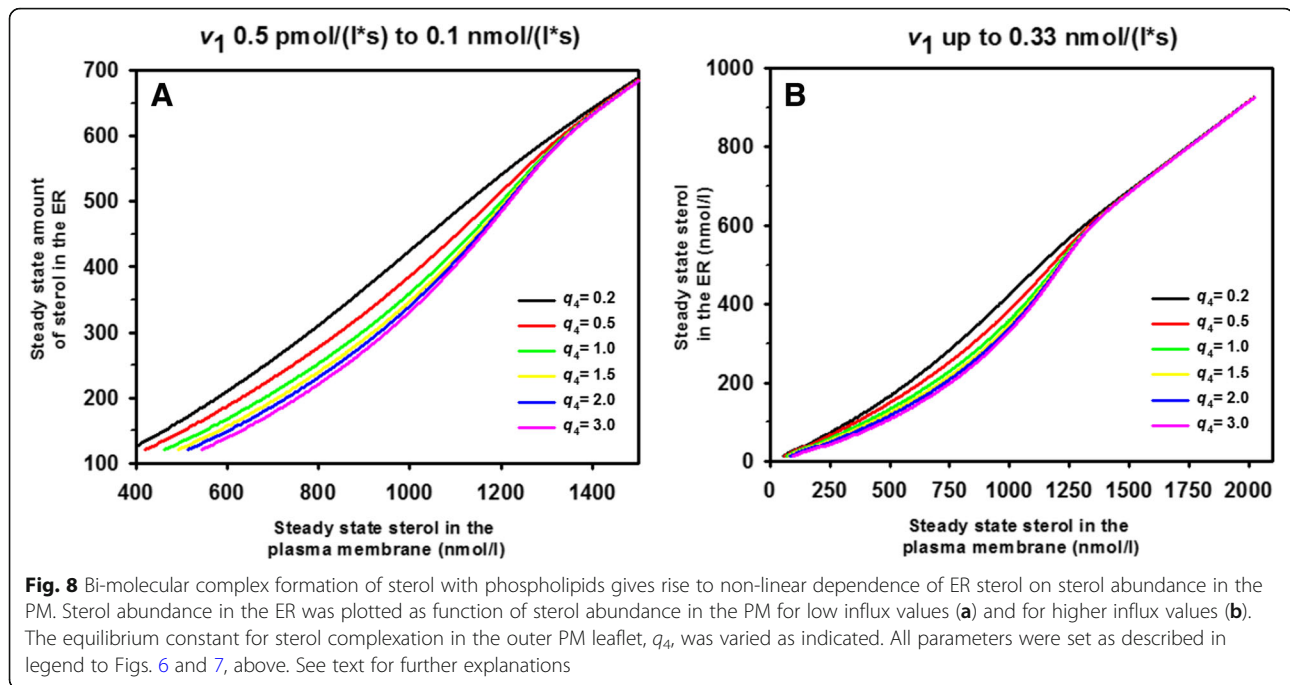
Sterol-phospholipid complexes cause a threshold-like dependence of the ER sterol pool size on PM sterol

Increased cholesterol in the PM of mammalian cells triggers several physiological responses in the ER above certain threshold values (reviewed in [8, 14]). For example, cholesterol's concentration in the ER depends non-linearly on that in the PM, and all of cholesterol added to cells beyond complexing capacity of the PM moves to the cytoplasmic membranes in fibroblasts [18, 41, 67, 68]. Activation of ACAT which esterifies cholesterol for storage in LDs in macrophages, takes also place upon expanding cholesterol levels beyond some threshold value, and that has been shown to be accompanied by rapid sterol influx from the PM [17, 43, 69]. Our bi-molecular model reconciles such observations (Fig. 8): for certain parameter combinations we found a steep rise in ER sterol once sterol levels in the PM passed some threshold value due to increasing sterol influx, ν_1 (i.e., for strong preference of complex formation; $q_4, q_5 \geq 10$, not shown). Thus, our model can describe threshold-like responses, but unfortunately, for such parameters, the steady state sterol ratio between PM and ER could not reconcile the experimentally determined 70:30 distribution in yeast. Thus, extreme threshold effects are either not present in the yeast system or require extensions of our model, i.e., probably cooperative phospholipid-sterol interactions would need to be included to account for that in a more physiological range of parameters. However, since the algebra gets more involved and strong thresholds have not been observed for yeast so far, this has not been considered further. Furthermore, the steepness of the experimentally observed threshold effect depends not only on the sterol complexing capability of the involved lipid species but also to some extent on the method used for threshold detection. That is, protein sensors, like perfringolysin or anthrolysin show highly cooperative membrane binding once sterol mole fractions in the bilayer exceed some threshold values [18, 59, 70]. Thus, the extent of non-linearity of a given response might depend on the experimental system and the method of its interrogation.

For parameters reconciling all experimental observations in the yeast system, the non-linear rise in ER sterol upon increase in PM sterol is predicted to be milder (Fig. 8a). Interestingly, this non-linear dependence of ER sterol abundance on sterol in the PM is only seen for low sterol influx values, where the hyperbolic sterol complex formation dominates. Plotting ER sterol as function of PM sterol over a larger range of sterol influx values reveals that this threshold actually describes a transition (Fig. 8b): for low sterol influx, complex formation can keep up with incoming new sterol. Once all binding phospholipids are consumed, i.e., beyond the stoichiometric capacity of complex formation, ER sterol depends linearly on PM sterol (Fig. 8b, beyond ca. $1.4 \mu\text{mol/l}$ PM sterol). This is, because from this point on each newly imported sterol molecule only feeds into the active sterol as the complexation capacity of the PM has been exceeded. Accordingly, we see a linear relationship between ER and PM sterol for larger sterol influx, ν_1 . The latter has – to our knowledge – not been reported, yet; neither in mammalian cells nor in yeast. This can have two reasons; first, steady state experiments are rarely carried out, even though this is in principal straightforward in yeast bearing a $\Delta hem1$ mutation, as outlined above. Instead, many experiments are carried out after membrane fractionation, e.g., reports using cholesterol-binding cytolysin derivatives or those involving radioactive sterols [9, 18, 70]. Such experiments can result in thermodynamic equilibration of pool sizes such that they cannot be compared directly to the steady state analysis presented here. Second, cells might avoid exceeding the threshold for active sterol too far and initiate homeostatic mechanisms to reset active sterol pool sizes below the threshold value [18, 59].

Discussion

The majority of cholesterol or ergosterol resides in the PM with low sterol abundance in the ER at steady state [14, 18, 20, 31, 41]. Recent studies in mammalian cells and yeast have shown that the majority of sterols in the PM reside in its inner leaflet [31, 71, 72]. However, some earlier studies report sterol enrichment in the outer compared to the inner leaflet, as recently reviewed in [73]. Technical challenges in measuring sterol distribution in the PM exactly have been suggested to be responsible for such discrepancies [31, 71, 73]. Our steady state sterol transport model predicts that other factors such as varying sterol import flux, cytoplasmic sterol release and rate of sterol esterification in the ER can impact the abundance and transbilayer distribution of ergosterol in the yeast PM. Sterols in the PM can rapidly equilibrate with the ER and other organelles via non-vesicular transport, both in mammalian cells [74–76] and in yeast [9, 20, 27, 29]. The magnitude of non-



vesicular sterol transfer from the PM can act as homeostatic mechanism for sterol abundance not only in the ER but also in recycling endosomes and lysosomes, which both have been shown to equilibrate their sterol pools rapidly with that in the PM [77–80]. Analogs of cholesterol and ergosterol show also fast transbilayer migration (flip-flop) in most model membrane studies [32, 33, 81, 82]. It is ad hoc not clear, how such strong sterol gradients between membranes or between their two leaflets can be maintained in the presence of high sterol fluxes. Here, we have used a mathematical approach and developed a simple steady state model to understand the key features of sterol flux across the yeast PM, thereby explaining apparently contradicting observations.

Conclusions and future perspectives

Key predictions of our model analysis are:

1. Influx of sterol into yeast cells under anaerobic growth conditions via ABC transporters sets the rates for sterol flip-flop across the PM, non-vesicular sterol transport to the ER and sterol esterification at steady state (i.e., there is only one non-equilibrium flux, $v_1 = J$, at steady state).
2. The attainable transbilayer sterol asymmetry at steady state is always (slightly) smaller than the equilibrium ratio (Fig. 2). Sterol esterification in the ER controls cytoplasmic sterol release and thereby

impacts sterol abundance and transbilayer distribution in the PM.

3. The steady state flux is an exponentially decaying function of the non-equilibrium chemical potential difference of sterol between both PM leaflets (Fig. 3). Thus, apart from ATP-dependent sterol import, ATP-consuming sterol esterification by Are2 in the ER keeps the system out of equilibrium, thereby exerting metabolic control over cellular sterol homeostasis.
4. Rapid sterol exchange between both PM leaflets (Fig. 4) and between PM and ER (Fig. 5) can be accounted for by a 2-pool model, in which sterol exists free for exchange ('active') or in complexes with phospholipids or proteins in both membranes.
5. For equal sterol flip-flop rates, enrichment of ergosterol in one PM leaflet requires its preferred complex formation in that leaflet (Fig. 5). In fact, the concentration of free, non-complexed sterol is larger in the outer than in the inner PM leaflet to ensure net transfer in the import direction. As a consequence, experimental methods which primarily detect free, non-complexed sterol could misinterpret the transbilayer distribution of sterols in the PM. The abundance of sterol binding partners, such as saturated phospholipids, determines the attainable sterol asymmetry in the PM.
6. Sterol abundance in the cells and their membranes increases hyperbolically for low influx rates due to formation of sterol-phospholipid complexes (Fig. 6).

For higher import rates, the complex forming capability of the PM is exceeded, and a linear relationship between sterol abundance and influx becomes apparent.

7. The steady state ratio of sterol between both PM leaflets as well as between the PM and ER is predicted to dependent in a non-linear manner on activity or abundance of Aus1/Pdr11 in the PM and Are2 in the ER (Fig. 7). Once the sterol influx exceeds the capacity of sterol complex formation in the PM, changes of import efficiency do not affect sterol distributions significantly.
8. Complex formation leads to a non-linear increase in sterol content of the ER as function of sterol in the PM (Fig. 8). For high sterol influx, a linear relationship between PM and ER sterol is re-established, as only active (free) sterol contributes to steady state flux between both compartments.

These are testable predictions for future experiments, in which the steady state sterol distribution between both PM leaflets as well as between PM and ER is assessed, e.g. using fluorescence imaging of the close ergosterol analog DHE. By varying the abundance of Aus1/Pdr11, whose expression is under control of the transcription factor Upc2 [65], one will be able to determine the regulatory mechanisms underlying sterol import under anaerobic growth conditions in yeast. Transport-coupled esterification of DHE in the ER and its storage in LDs can be studied by a combination of biochemical and imaging experiments in cells with varying expression level of Are2 [27]. This should translate into varying rate constant k_7 of our model. By varying the abundance and/or distribution of sphingolipids and PS using chemical inhibitors, mutants of enzymes involved in lipid synthesis or knock-outs of PM phospholipid flippases, one will be able to determine, to what extent lipids contribute to sterol complex formation in the PM and thereby to maintenance of the sterol gradient between PM and ER. Furthermore, a variety of sterol or sphingolipid sensing cytolysins could be expressed as fluorescence-tagged constructs and studied in concert with DHE by multi-color fluorescence microscopy [83]. Assuming passage of the low-molecular weight proteins through the yeast cell wall, their binding to the outer PM leaflet could be even studied after appropriate fluorescence labeling. This could even allow for dissection of sphingolipid-sterol interactions in the outer PM leaflet of yeast cells using ostreolysin A, a cytolysin recently described as molecular sensor for sphingomyelin-cholesterol complexes [16]. Combining such experiments with chemical inhibition of biosynthesis of some lipid species will provide valuable insight into sterol interactions in native membranes. This could allow for a direct test of

another hypothesis, namely that ergosterol is supposed to segregate from tightly packed sphingolipids in the yeast PM [57].

An extension of the model in future studies could include accounting for cooperative interactions between sterol and phospholipid in complexes, which could even better describe threshold-like transitions in sterol release from the PM, as observed for mammalian cells [17, 19, 41, 43, 44]. Cooperative sterol complexation has been suggested based on cholesterol-phospholipid phase diagrams in model lipid systems, and such a process could be included in our model by introducing a new parameter for oligomerization [15, 52, 55]. In addition, the stoichiometry of complex formation between sterol and phospholipid might be varied using $m, n > 1$ in the rates v_4, v_5 and v_6 (Eq. 35), as other stoichiometries than 1:1 have been suggested in several studies [15, 54, 63, 84]. Such an extension will complicate the algebra significantly calling for numerical solutions, but it might be an approach to describe highly non-linear flux responses for realistic parameter combinations in both, yeast and mammalian cells.

Finally, it should not go unnoticed, that our model is a simplification of the real biochemical scenario, and that many aspects of the complex problem of intracellular cholesterol transport are not considered. Non-steady state sterol biosynthesis and steryl ester hydrolysis will certainly contribute to sterol homeostasis but have not been considered in the model presented here. Allosteric activation of sterol esterification by sterol abundance in the ER is likely to play a role as well, but has not been included in our model, either. Yeast and mammalian cells have to operate under a variety of environmental conditions, making that their homeostatic control mechanisms have to deal with several inputs, for example, by adjusting the expression of proteins in a given metabolic pathway. Anaerobic sterol uptake in yeast is under tight control of the expression factor Upc2, which responds to a decrease in cytosolic ergosterol by translocation to the nucleus for initiating expression of Aus1/Pdr11 and other proteins [65]. Such feedback mechanisms have not been considered here, but could be included in future studies. Similarly, transport and metabolism of sterols and other lipids can change throughout the yeast cell cycle, for example prior to and after diauxic shift or during growth resumption and in the stationary state [85, 86]. Also, steryl esters in LDs can be utilized by other pathways, such as by ingestion into the vacuole (the yeast lysosome) during starvation in a process called lipophagy [87, 88]. Metabolic adjustments such as utilization of LDs are carried out in concert with the PM and the vacuole via target of rapamycin 1 and 2 (TORC1 and TORC2), two kinases regulating metabolic programs under various environmental cues [86, 89]. An important but challenging strategy could be to include these

aspects into our model in the future. Finally, many of the rate constants used here have been estimated based on literature values, which cannot replace a proper parametrization of the model. For that, one would need to carry out kinetic experiments and fit time-dependent solutions of the model to the data. This will be attempted in future studies.

Parameter symbol	Parameter function	Explored parameter values	Lipid pool symbol	Lipid pool definition
$v_1 = J$	Sterol influx at steady state	$0.5 \text{ pmol} \cdot \text{l}^{-1} \cdot \text{s}^{-1}$ to $0.1 \text{ nmol} \cdot \text{l}^{-1} \cdot \text{s}^{-1}$	S_1^{eq}	Sterol in outer PM leaflet at equilibrium
V_{max}	Maximal activity of Aus1/Pdr11	$0.5 \text{ pmol} \cdot \text{l}^{-1} \cdot \text{s}^{-1}$ to $0.33 \text{ nmol} \cdot \text{l}^{-1} \cdot \text{s}^{-1}$	S_2^{eq}	Sterol in inner PM leaflet at equilibrium
E_T	Concentration of Aus1/Pdr11	$0.2 \text{ nmol} \cdot \text{l}^{-1}$	\bar{S}_1	Freely mobile sterol pool in outer PM leaflet at steady state
$k_M = \frac{m_1+m_2}{m_1}$	Michaelis-Menten constant of sterol import	NA	\bar{S}_2	Freely mobile sterol pool in inner PM leaflet at steady state
k_1	Import rate constant	NA	\bar{S}_3	Freely mobile sterol pool in ER at steady state
k_{-1}	Export rate constant	NA	\bar{C}_1	Sterol-phospholipid complexes in outer PM leaflet at steady state
k_2	Flip rate constant	$0.1-10 \text{ s}^{-1}$	\bar{C}_2	Sterol-phospholipid complexes in inner PM leaflet at steady state
k_{-2}	Flop rate constant	$0.1-1 \text{ s}^{-1}$	\bar{C}_3	Sterol-phospholipid complexes in ER at steady state
k_3	Rate constant for non-vesicular transport	$0.01-1 \text{ s}^{-1}$	P_{T1}	Phospholipid available for complexes in outer PM leaflet
k_4	Rate constant for sterol-phl. complexation in outer PM leaflet	$0.001-1 \text{ s}^{-1}$	P_{T2}	Phospholipid available for complexes in inner PM leaflet
k_{-4}	Rate constant for sterol-phl. dissociation in	$0.001-1 \text{ s}^{-1}$	P_{T3}	Phospholipid available for complexes in

Conclusions and future perspectives (Continued)

Parameter symbol	Parameter function	Explored parameter values	Lipid pool symbol	Lipid pool definition
	outer PM leaflet			ER
k_5	Rate constant for sterol-phl. complexation in inner PM leaflet	$0.001-1 \text{ s}^{-1}$	$S_T = PM_T$	Total sterol in PM
k_{-5}	Rate constant for sterol-phl. dissociation in inner PM leaflet	$0.001-1 \text{ s}^{-1}$	ER_T	Total sterol in ER
k_6	Rate constant for sterol-phl. complexation in ER	$0.001-1 \text{ s}^{-1}$	Q	Ratio of free sterol between PM leaflets in Eq. 1
k_{-6}	Rate constant for sterol-phl. dissociation in ER	$0.001-1 \text{ s}^{-1}$	Q'	Ratio of free sterol between PM leaflets in Eq. 44, 5
k_7	Rate constant for sterol esterification in ER	$0.001-1 \text{ s}^{-1}$	S_T^0	Total sterol in outer PM leaflet
q_2	Equilibrium constant for sterol flip-flop	$0.01-10$	S_T^f	Total sterol in inner PM leaflet
q_3	Equilibrium constant for sterol transport between PM and ER	$0.01-10$	S_0	Total sterol in medium
q_4	Equilibrium constant for complexes in outer PM leaflet	$0.01-10$		
q_5	Equilibrium constant for complexes in inner PM leaflet	$0.01-10$		
q_6	Equilibrium constant for complexes in ER	$0.01-1.0$		
r	Fractional rate constant for sterol esterification in ER	NA		
$C_{k_i}^J$	Flux control coefficient with respect to parameter k_i	1		
$C_{k_i}^{S_j}$	Concentration	1		

Conclusions and future perspectives (Continued)

Parameter symbol	Parameter function	Explored parameter values	Lipid pool symbol	Lipid pool definition
	control coefficient with respect to parameter k_i			

Abbreviations

DHE: Dehydroergosterol; ER: Endoplasmic reticulum; ERC: Endocytic recycling compartment; LDs: Lipid droplets; MCS: Membrane contact sites; OSBP: Oxysterol binding protein; Osh: OSBP homologs in yeast; PM: Plasma membrane; PS: Phosphatidylserine; STPs: Sterol transport proteins

Acknowledgements

Not applicable

Authors' contributions

DW designed the study, carried out the model analysis and wrote the paper. The author read and approved the final manuscript.

Funding

DW acknowledges support from the Villum Center for Bioanalytical Sciences.

Availability of data and materials

The datasets used and/or analyzed during the current study are available from author on request.

Ethics approval and consent to participate

Not applicable.

Consent for publication

Not applicable.

Competing interests

The author declares that he has no competing interests.

Received: 11 March 2019 Accepted: 15 July 2019

Published online: 15 August 2019

References

- Wüstner D. Intracellular cholesterol transport. In: Ehnholm C, editor. Cellular lipid metabolism. Berlin: Springer Press; 2009. p. 157–90.
- Mesmin B, Maxfield FR. Intracellular sterol dynamics. *Biochim Biophys Acta*. 2009;1791:636–45.
- Maxfield FR, Tabas I. Role of cholesterol and lipid organization in disease. *Nature*. 2005;438:612–21.
- Maxfield FR, Wüstner D. Intracellular cholesterol transport. *J Clin Invest*. 2002;110:891–8.
- Dittman JS, Menon AK. Speed limits for nonvesicular intracellular sterol transport. *Trends Biochem Sci*. 2017;42:90–7.
- Estronca LM, Moreno MJ, Vaz WL. Kinetics and thermodynamics of the association of dehydroergosterol with lipid bilayer membranes. *Biophys J*. 2007;93:4244–53.
- McLean LR, Phillips MC. Mechanism of cholesterol and phosphatidylcholine exchange or transfer between unilamellar vesicles. *Biochemistry*. 1981;20:2893–900.
- Wüstner D, Solanko KA. How cholesterol interacts with proteins and lipids during its intracellular transport. *Biochim Biophys Acta*. 2015;1848:2188–99.
- Baumann NA, Sullivan DP, Ohvo-Rekila H, Simonot C, Pottekat A, Klaassen Z, Beh CT, Menon AK. Transport of newly synthesized sterol to the sterol-enriched plasma membrane occurs via nonvesicular equilibration. *Biochemistry*. 2005;44:5816–26.
- Maxfield FR, Menon AK. Intracellular sterol transport and distribution. *Curr Opin Cell Biol*. 2006;18:379–85.
- Schulz TA, Choi MG, Raychaudhuri S, Mears JA, Ghirlando R, Hinshaw JE, Prinz WA. Lipid-regulated sterol transfer between closely apposed membranes by oxysterol-binding protein homologues. *J Cell Biol*. 2009;187:889–903.
- Sturley SL. Conservation of eukaryotic sterol homeostasis: new insights from studies in budding yeast. *Biochim Biophys Acta*. 2000;1529:155–63.
- Menon AK. Sterol gradients in cells. *Curr Opin Cell Biol*. 2018;53:37–43.
- Lange Y, Steck TL. Active membrane cholesterol as a physiological effector. *Chem Phys Lipids*. 2016;199:74–93.
- Radhakrishnan A, McConnell HM. Chemical activity of cholesterol in membranes. *Biochemistry*. 2000;39:8119–24.
- Endapally S, Frias D, Grzemska M, Gay A, Tomchick DR, Radhakrishnan A. Molecular discrimination between two conformations of sphingomyelin in plasma membranes. *Cell*. 2019;176:1040–1053.e1017.
- Xu XX, Tabas I. Lipoproteins activate acyl-coenzyme a:cholesterol acyltransferase in macrophages only after cellular cholesterol pools are expanded to a critical threshold level. *J Biol Chem*. 1991;266:17040–8.
- Sokolov A, Radhakrishnan A. Accessibility of cholesterol in endoplasmic reticulum membranes and activation of SREBP-2 switch abruptly at a common cholesterol threshold. *J Biol Chem*. 2010;285:29480–90.
- Okwu AK, Xu XX, Shiratori Y, Tabas I. Regulation of the threshold for lipoprotein-induced acyl-CoA:cholesterol O-acyltransferase stimulation in macrophages by cellular sphingomyelin content. *J Lipid Res*. 1994;35:644–55.
- Sullivan DP, Ohvo-Rekila H, Baumann NA, Beh CT, Menon AK. Sterol trafficking between the endoplasmic reticulum and plasma membrane in yeast. *Biochem Soc Trans*. 2006;34:356–8.
- Li Y, Prinz WA. ATP-binding cassette (ABC) transporters mediate nonvesicular, raft-modulated sterol movement from the plasma membrane to the endoplasmic reticulum. *J Biol Chem*. 2004;279:45226–34.
- Scheidt HA, Müller P, Herrmann A, Huster D. The potential of fluorescent and spin-labeled steroid analogs to mimic natural cholesterol. *J Biol Chem*. 2003;278:45563–9.
- Garvik O, Benediktson P, Simonsen AC, Ipsen JH, Wüstner D. The fluorescent cholesterol analog dehydroergosterol induces liquid-ordered domains in model membranes. *Chem Phys Lipids*. 2009;159:114–8.
- Kohut P, Wüstner D, Hronská L, Kuchler K, Hapala I, Valachovic M. The role of ABC proteins Aus1p and Pdr1p in the uptake of external sterols in yeast: Dehydroergosterol fluorescence study. *Biochem Biophys Res Commun*. 2011;404:233–8.
- Alimardani P, Régnacq M, Moreau-Vauzelle C, Ferreira T, Rognon T, Blondin B, Bergès T. SUT1-promoted sterol uptake involves the ABC transporter Aus1 and the mannoprotein Dan1 whose synergistic action is sufficient for this process. *Biochem J*. 2004;381:195–202.
- Chauhan N, Jentsch JA, Menon AK. Measurement of Intracellular Sterol Transport in Yeast. In: Drin G, (eds). *Intracellular Lipid Transport*. New York: Humana Press; 2019.
- Georgiev AG, Sullivan DP, Kersting MC, Dittman JS, Beh CT, Menon AK. Osh proteins regulate membrane sterol organization but are not required for sterol movement between the ER and PM. *Traffic*. 2011;12:1341–55.
- Georgiev AG, Johansen J, Ramanathan VD, Sere YY, Beh CT, Menon AK. Arv1 regulates PM and ER membrane structure and homeostasis but is dispensable for intracellular sterol transport. *Traffic*. 2013;14:912–21.
- Gatta AT, Wong LH, Sere YY, Calderón-Noreña DM, Cockcroft S, Menon AK, Levine TP. A new family of StART domain proteins at membrane contact sites has a role in ER-PM sterol transport. *Elife*. 2015;4. <https://doi.org/10.7554/eLife.07253>.
- Quon E, Sere YY, Chauhan N, Johansen J, Sullivan DP, Dittman JS, Rice WJ, Chan RB, Di Paolo G, Beh CT, Menon AK. Endoplasmic reticulum-plasma membrane contact sites integrate sterol and phospholipid regulation. *PLoS Biol*. 2018;16:e2003864.
- Solanko LM, Sullivan DP, Sere YY, Szomek M, Lunding A, Solanko KA, Pizovic A, Stanchev LD, Pomorski TG, Menon AK, Wüstner D. Ergosterol is mainly located in the cytoplasmic leaflet of the yeast plasma membrane. *Traffic*. 2018;19:198–214.
- John K, Kubelt J, Muller P, Wüstner D, Herrmann A. Rapid transbilayer movement of the fluorescent sterol dehydroergosterol in lipid membranes. *Biophys J*. 2002;83:1525–34.
- Müller P, Herrmann A. Rapid transbilayer movement of spin-labeled steroids in human erythrocytes and in liposomes. *Biophys J*. 2002;82:1418–28.
- Beard DA, Qian H. Chemical biophysics : quantitative analysis of cellular systems. Cambridge: Cambridge University Press; 2008.

35. Marek M, Silvestro D, Fredslund MD, Andersen TG, Pomorski TG. Serum albumin promotes ATP-binding cassette transporter-dependent sterol uptake in yeast. *FEMS Yeast Res.* 2014;14:1223–33.
36. Reiner S, Micolod D, Zellnig G, Schneider R. A genomewide screen reveals a role of mitochondria in anaerobic uptake of sterols in yeast. *Mol Biol Cell.* 2006;17:90–103.
37. Heinrich R, Schuster S. The regulation of cellular processes. New York: Chapman & Hall; 1996. p. 123–34.
38. Laub KR, Marek M, Stanchev LD, Herrera SA, Kanashova T, Bourmaud A, Dittmar G, Gunther Pomorski T. Purification and characterisation of the yeast plasma membrane ATP binding cassette transporter Pdr11p. *PLoS One.* 2017;12:e0184236.
39. Marek M, Milles S, Schreiber G, Dalek DL, Dittmar G, Herrmann A, Muller P, Pomorski TG. The yeast plasma membrane ATP binding cassette (ABC) transporter Aus1: purification, characterization, and the effect of lipids on its activity. *J Biol Chem.* 2011;286:21835–43.
40. Wüstner D, Lund FW, Röhrl C, Stangl H. Potential of BODIPY-cholesterol for analysis of cholesterol transport and diffusion in living cells. *Chem Phys Lipids.* 2015;194:12–28.
41. Lange Y, Ye J, Rigney M, Steck TL. Regulation of endoplasmic reticulum cholesterol by plasma membrane cholesterol. *J Lipid Res.* 1999;40:2264–70.
42. Lange Y, Ye J, Steck TL. How cholesterol homeostasis is regulated by plasma membrane cholesterol in excess of phospholipids. *Proc Natl Acad Sci U S A.* 2004;101:11664–7.
43. Wüstner D, Mondal M, Tabas I, Maxfield FR. Direct observation of rapid internalization and intracellular transport of sterol by macrophage foam cells. *Traffic.* 2005;6:396–412.
44. Slotte JP, Bierman EL. Depletion of plasma-membrane sphingomyelin rapidly alters the distribution of cholesterol between plasma membranes and intracellular cholesterol pools in cultured fibroblasts. *Biochem J.* 1988; 250:653–8.
45. Giang H, Schick M. How cholesterol could be drawn to the cytoplasmic leaf of the plasma membrane by phosphatidylethanolamine. *Biophys J.* 2014; 107:2337–44.
46. Qian H, Beard DA, Liang SD. Stoichiometric network theory for nonequilibrium biochemical systems. *Eur J Biochem.* 2003;270:415–21.
47. Steck TL, Lange Y. Transverse distribution of plasma membrane bilayer cholesterol: picking sides. *Traffic.* 2018;19:750–60.
48. Balakrishnan L, Venter H, Shilling RA, van Veen HW. Reversible transport by the ATP-binding cassette multidrug export pump LmrA: ATP synthesis at the expense of downhill ethidium uptake. *J Biol Chem.* 2004;279:11273–80.
49. Grossmann N, Vakkasoglu AS, Hulpke S, Abele R, Gaudet R, Tampe R. Mechanistic determinants of the directionality and energetics of active export by a heterodimeric ABC transporter. *Nat Commun.* 2014;5:5419.
50. Steck TL, Lange Y. Cell cholesterol homeostasis: mediation by active cholesterol. *Trends Cell Biol.* 2010;20:680–7.
51. Ijäs HK, Lönnfors M, Nyholm TKM. Sterol affinity for phospholipid bilayers is influenced by hydrophobic matching between lipids and transmembrane peptides. *Biochim Biophys Acta.* 2013;1828:932–7.
52. Radhakrishnan A, McConnell HM. Condensed complexes of cholesterol and phospholipids. *Biophys J.* 1999;77:1507–17.
53. Radhakrishnan A, Anderson TG, McConnell HM. Condensed complexes, rafts, and the chemical activity of cholesterol in membranes. *Proc Natl Acad Sci U S A.* 2000;97:12422–7.
54. Radhakrishnan A, Li XM, Brown RE, McConnell HM. Stoichiometry of cholesterol-sphingomyelin condensed complexes in monolayers. *Biochim Biophys Acta.* 2001;1511:1–6.
55. Radhakrishnan A, McConnell H. Condensed complexes in vesicles containing cholesterol and phospholipids. *Proc Natl Acad Sci U S A.* 2005;102:12662–6.
56. Chen Y, Yu L. Recent progress in autophagic lysosome reformation. *Traffic.* 2017;18:358–61.
57. Aresta-Branco F, Cordeiro AM, Marinho HS, Cyrne L, Antunes F, de Almeida RF. Gel domains in the plasma membrane of *Saccharomyces cerevisiae*: highly ordered, ergosterol-free, and sphingolipid-enriched lipid rafts. *J Biol Chem.* 2011;286:5043–54.
58. Hiramata T, Lu SM, Kay JG, Maekawa M, Kozlov MM, Grinstein S, Fairn GD. Membrane curvature induced by proximity of anionic phospholipids can initiate endocytosis. *Nat Commun.* 2017;8:1393.
59. Das A, Brown MS, Anderson DD, Goldstein JL, Radhakrishnan A. Three pools of plasma membrane cholesterol and their relation to cholesterol homeostasis. *ELife.* 2014;3:e02882.
60. Infante RE, Radhakrishnan A. Continuous transport of a small fraction of plasma membrane cholesterol to endoplasmic reticulum regulates total cellular cholesterol. *ELife.* 2017;6. <https://doi.org/10.7554/eLife.25466>.
61. Wattenberg BW, Silbert DF. Sterol partitioning among intracellular membranes. Testing a model for cellular sterol distribution. *J Biol Chem.* 1983;258:2284–9.
62. McConnell HM, Radhakrishnan A. Condensed complexes of cholesterol and phospholipids. *Biochim Biophys Acta.* 2003;1610:159–73.
63. Lange Y, Tabei SM, Ye J, Steck TL. Stability and stoichiometry of bilayer phospholipid-cholesterol complexes: relationship to cellular sterol distribution and homeostasis. *Biochemistry.* 2013;52:6950–9.
64. Wilcox LJ, Balderes DA, Wharton B, Tinkenberg AH, Rao G, Sturley SL. Transcriptional profiling identifies two members of the ATP-binding cassette transporter superfamily required for sterol uptake in yeast. *J Biol Chem.* 2002;277:32466–72.
65. Yang H, Tong J, Lee CW, Ha S, Eom SH, Im YJ. Structural mechanism of ergosterol regulation by fungal sterol transcription factor Upc2. *Nat Commun.* 2015;6:6129.
66. Gulati S, Balderes D, Kim C, Guo ZA, Wilcox L, Area-Gomez E, Snider J, Wolinski H, Stagljar I, Granato JT, et al. ATP-binding cassette transporters and sterol O-acyltransferases interact at membrane microdomains to modulate sterol uptake and esterification. *FASEB J.* 2015;29:4682–94.
67. Lange Y, Ory DS, Ye J, Lanier MH, Hsu FF, Steck TL. Effectors of rapid homeostatic responses of endoplasmic reticulum cholesterol and 3-hydroxy-3-methylglutaryl-CoA reductase. *J Biol Chem.* 2008;283:1445–55.
68. Lange Y, Ye J, Steck TL. Essentially all excess fibroblast cholesterol moves from plasma membranes to intracellular compartments. *PLoS One.* 2014;9:e98482.
69. Li Y, Ge M, Ciani L, Kuriakose G, Westover EJ, Dura M, Covey DF, Freed JH, Maxfield FR, Lytton J, Tabas I. Enrichment of endoplasmic reticulum with cholesterol inhibits sarcoplasmic-endoplasmic reticulum calcium ATPase-2b activity in parallel with increased order of membrane lipids: implications for depletion of endoplasmic reticulum calcium stores and apoptosis in cholesterol-loaded macrophages. *J Biol Chem.* 2004;279:37030–9.
70. Das A, Goldstein JL, Anderson DD, Brown MS, Radhakrishnan A. Use of mutant 125I-perfringolysin O to probe transport and organization of cholesterol in membranes of animal cells. *Proc Natl Acad Sci.* 2013; 110:10580–5.
71. Mondal M, Mesmin B, Mukherjee S, Maxfield FR. Sterols are mainly in the cytoplasmic leaflet of the plasma membrane and the endocytic recycling compartment in CHO cells. *Mol Biol Cell.* 2009;20:581–8.
72. Courtney KC, Pezeshkian W, Raghupathy R, Zhang C, Darbyson A, Ipsen JH, Ford DA, Khandelia H, Presley JF, Zha X. C24 sphingolipids govern the transbilayer asymmetry of cholesterol and lateral organization of model and live-cell plasma membranes. *Cell Rep.* 2018;24:1037–49.
73. Kaphishnikov S, Leiserowitz L, Yang Y, Cloetens P, Pereira E, Awamu Ndonglack F, Matuschewski K, Als-Nielsen J. Biochemistry of malaria parasite infected red blood cells by X-ray microscopy. *Sci Rep.* 2017;7:802.
74. Kaplan MR, Simoni RD. Transport of cholesterol from the endoplasmic reticulum to the plasma membrane. *J Cell Biol.* 1985;101:446–53.
75. Mesmin B, Pipalia NH, Lund FW, Ramlall TF, Sokolov A, Eliezer D, Maxfield FR. STARD4 abundance regulates sterol transport and sensing. *Mol Biol Cell.* 2011;22:4004–15.
76. Sandhu J, Li S, Fairall L, Pfisterer SG, Gurnett JE, Xiao X, Weston TA, Vashi D, Ferrari A, Orozco JL, et al. Aster proteins facilitate nonvesicular plasma membrane to ER cholesterol transport in mammalian cells. *Cell.* 2018;175(2): 514–529.e20.
77. Hao M, Lin SX, Karylowski OJ, Wüstner D, McGraw TE, Maxfield FR. Vesicular and non-vesicular sterol transport in living cells. The endocytic recycling compartment is a major sterol storage organelle. *J Biol Chem.* 2002;277:609–17.
78. Lange Y, Ye J, Steck TL. Circulation of cholesterol between lysosomes and the plasma membrane. *J Biol Chem.* 1998;273:18915–22.
79. Berzina Z, Solanko LM, Mehadi AS, Jensen MLV, Lund FW, Modzel M, Szomek M, Solanko KA, Dupont A, Nielsen GK, et al. Niemann-Pick C2 protein regulates sterol transport between plasma membrane and late endosomes in human fibroblasts. *Chem Phys Lipids.* 2018;213:48–61.

80. Castellano BM, Thelen AM, Moldavski O, Feltes M, van der Welle RE, Mydock-McGrane L, Jiang X, van Eijkeren RJ, Davis OB, Louie SM, et al. Lysosomal cholesterol activates mTORC1 via an SLC38A9-Niemann-Pick C1 signaling complex. *Science*. 2017;355:1306–11.
81. Steck TL, Ye J, Lange Y. Probing red cell membrane cholesterol movement with cyclodextrin. *Biophys J*. 2002;83:2118–25.
82. Leventis R, Silvius JR. Use of cyclodextrins to monitor transbilayer movement and differential lipid affinities of cholesterol. *Biophys J*. 2001; 81:2257–67.
83. Maekawa M, Fairm GD. Complementary probes reveal that phosphatidylserine is required for the proper transbilayer distribution of cholesterol. *J Cell Sci*. 2015;128:1422–33.
84. Okonogi TM, Radhakrishnan A, McConnell HM. Two fatty acids can replace one phospholipid in condensed complexes with cholesterol. *Biochim Biophys Acta*. 2002;1564:1–4.
85. Casanovas A, Sprenger RR, Tarasov K, Ruckerbauer DE, Hannibal-Bach HK, Zanghellini J, Jensen ON, Ejsing CS. Quantitative analysis of proteome and lipidome dynamics reveals functional regulation of global lipid metabolism. *Chem Biol*. 2015;22:412–25.
86. Ouahoud S, Fiet MD, Martinez-Montanes F, Ejsing CS, Kuss O, Roden M, Markgraf DF. Lipid droplet consumption is functionally coupled to vacuole homeostasis independent of lipophagy. *J Cell Sci*. 2018;131. <https://doi.org/10.1242/jcs.213876>.
87. Wang CW, Miao YH, Chang YS. A sterol-enriched vacuolar microdomain mediates stationary phase lipophagy in budding yeast. *J Cell Biol*. 2014; 206:357–66.
88. Shpilka T, Welter E, Borovsky N, Amar N, Mari M, Reggiori F, Elazar Z. Lipid droplets and their component triglycerides and steryl esters regulate autophagosome biogenesis. *EMBO J*. 2015;34:2117–31.
89. Horenkamp FA, Valverde DP, Nunnari J, Reinisch KM. Molecular basis for sterol transport by StART-like lipid transfer domains. *EMBO J*. 2018;37. <https://doi.org/10.15252/embj.201798002>.

Publisher's Note

Springer Nature remains neutral with regard to jurisdictional claims in published maps and institutional affiliations.

Ready to submit your research? Choose BMC and benefit from:

- fast, convenient online submission
- thorough peer review by experienced researchers in your field
- rapid publication on acceptance
- support for research data, including large and complex data types
- gold Open Access which fosters wider collaboration and increased citations
- maximum visibility for your research: over 100M website views per year

At BMC, research is always in progress.

Learn more biomedcentral.com/submissions

